

UNIVERSIDADE FEDERAL DO RIO GRANDE DO SUL  
FACULDADE DE ODONTOLOGIA  
DEPARTAMENTO DE ODONTOLOGIA CONSERVADORA  
PROGRAMA DE PÓS-GRADUAÇÃO EM ODONTOLOGIA

**FABIO ROCHA BOHNS**

**NANOTUBOS DE NITRETO DE BORO COMO CARGA EM UM INFILTRANTE  
RESINOSO**

PORTE ALEGRE

2017

**FABIO ROCHA BOHNS**

**NANOTUBOS DE NITRETO DE BORO COMO CARGA EM UM INFILTRANTE  
RESINOSO**

Dissertação de mestrado apresentada ao  
Programa de Pós-Graduação em  
Odontologia, da Universidade Federal do Rio  
Grande do Sul, como parte dos requisitos  
para a obtenção do título de Mestre em  
Clínica Odontológica.

Área de concentração: Materiais Dentários.

ORIENTADOR: SUSANA MARIA WERNER SAMUEL

PORTO ALEGRE

2017

CIP - Catalogação na Publicação

Bohns, Fabio Rocha  
Nanotubos de nitreto de boro como carga em um  
infiltrante resinoso / Fabio Rocha Bohns. -- 2017.  
63 f.  
Orientadora: Susana Maria Werner Samuel.

Dissertação (Mestrado) -- Universidade Federal do  
Rio Grande do Sul, Faculdade de Odontologia,  
Programa de Pós-Graduação em Odontologia, Porto  
Alegre, BR-RS, 2017.

1. nanotubos. 2. cáries dentárias. 3. esmalte  
dentário. 4. interações hidrófobas e hidrófilas. 5.  
análise de espectro, raman. I. Samuel, Susana Maria  
Werner, orient. II. Título.

Elaborada pelo Sistema de Geração Automática de Ficha Catalográfica da UFRGS com os  
dados fornecidos pelo(a) autor(a).

## **DEDICATÓRIA**

Dedico esse trabalho à **Anna Maria Valente**, ao **Paulo Arthur Hartmann Iop** e ao **Rafael Ferreira da Rosa**. Mesmo que não estejam presentes em carne e osso, sempre estarão nos meus pensamentos em cada novo passo dado.

## **AGRADECIMENTOS**

Ao meu pai, **Paulo Renato de Quadros Bohns**, por todo o apoio financeiro, pela companhia no assado do fim de semana, pelo chimarrão e por todos os puxões de orelha.

À minha mãe, **Tânia Rocha Bohns**, por novamente influenciar na minha escolha em continuar estudando.

À minha irmã, **Karina Rocha Bohns**, por todo o suporte e aconchego do lar que me proporcionou.

À minha irmã, **Rafaelle Rocha Bohns**, por toda influência e por ter me servido como espelho de empenho e luta.

Às minhas sobrinhas e sobrinho, **Laura Rocha Finkler, Marina Rocha Finkler e Pedro Bohns Guedes**.

Ao meu cunhado **Ricardo Guedes e família**, por sempre fazer me sentir em casa.

À minha família de **Pelotas (tios e primos)** e a que mora em **Santa Catarina (avós, tios e primos)**, que mesmo estando longe estão sempre presentes.

À minha namorada, **Camila Kops Ferreira**, por toda a calma, amizade, conselhos e por ter sido fundamental nesse meu último ano do mestrado.

À família **Kops Ferreira**, pelos momentos ótimos e incentivo.

Ao Prof. Dr. **Fabrício Mezzomo Collares**, por ter acreditado no meu potencial desde o inicio, pelos ensinamentos e por ter me acolhido na Faculdade de Odontologia.

Ao Prof. Dr. **Vicente Castelo Branco Leitune**, pelos ensinamentos, seriedade, competência e por ter me acolhido.

À Prof. Dra. **Susana Maria Werner Samuel**, pelo exemplo de profissional a ser seguido.

À Prof. Dra. **Carmem Beatriz Borges Fortes**, pela simpatia e dedicação.

Ao Prof. Dr. **Fabrício Aulo Ogliari**, por nunca ter me desencorajado de fazer um Mestrado fora da Eng. de Materiais.

À Dra. **Bruna Genari**, Dra. **Stéfani Rodrigues** e ao Dr. **Felipe Weidenbach Degrazia**, por todos os ensinamentos e auxílios.

Às minhas colegas de Mestrado **Carolina Jung Ferreira**, **Gabriela Balbinot**, **Isadora Garcia**, **Marla Cuppini** e **Patrícia Franken**, por terem sido as melhores, mais loucas, mais incríveis colegas possíveis e por terem respondido todas as minhas dúvidas de não dentista nesses dois anos e meio de convívio no LAMAD.

Aos colegas e equipe do Laboratório de Materiais Dentários (LAMAD): **Ana Laura**, **Ana Helena**, **Carolina Augusto**, **Douglas Paixão**, **Elisa Figueiredo**, **Fabio de Cesare**, **Fernanda Noal**, **Islam Bendary**, **Juliana Caletti**, **Juliana Walcher**, **Laisa Cruzetta**, **Lucas Bonfanti**, **Mariana Barreto**, **Mariele Mildner**, **Marília Paulus**, **Michele Stürmer**, **Nélio Dornelles**, **Priscila Schiroki**, **Rodrigo Tubelo**, **Rosemeri Pedroso**, **Tiago Herpich** e aos que recém chegaram.

À família que eu escolhi, **Leandro Zago, Gabriel Santos, Lisiane Assis Brasil, Lucca, Matheus Weber, Nicoli Friedrich, Renata Duarte, Talissa Rosário, Thiago Beresford e Vinicius Guerra**, por estarem sempre presentes, não importando a situação.

Aos amigos da faculdade, do colégio e da vida, **Alexandre Schumacher, Ana Carolina de Azevedo, André Camargo, André Ribeiro, André Willers, Angela Casaril, Birigui, Bruno Deki, Eric Quanz, Fausto, Giovani Ghiggi, Gabriel Borges, Jorge Lucas, Julia Brito, Katarine Rosso, Lucas Dias, Marciel Gaier, Maria Gabriela, Matheus Machado, Pedro de Oliveira, Rafael Levy, Ricardo Ritter, Rodrigo Ferreira, Romel Falcão, Tiago Iepsen, Thalles Gossling, Vicente Bordin, Xuby, Yumi** e os demais que não quero cometer o erro de esquecer algum.

Aos amigos do intercâmbio **Bruno Ferraz, Felipe Almeida, Gregório de Melo, Larissa Heinish e Ludimila Nakanami** (flat) e aos demais.

To my friends overseas **Alison Crosland, Matt Mackenzie, Michael Butlin, Sophie and Briony Rose**.

Ao meu pub favorito (**Lagom**), por sempre estar lá quando precisei descontrair, e ao **Lucas Bueno**, por sempre servir o *pint* perfeito.

A todo o **PPGODO** e faculdade de Odontologia da UFRGS.

Aos professores, técnicos e bolsistas que me ajudaram no **CME**, no departamento de **Física, LACER e LABIM**.

À **Universidade Federal do Rio Grande do Sul**, por ter me possibilitado realizar um sonho e dar mais um passo adiante na minha carreira.

A todos os professores pelos quais passei.

Obrigado.

*“If I have seen further it is by standing on the shoulders of Giants.”*

*Isaac Newton*

## RESUMO

O objetivo do presente estudo foi investigar as propriedades de um infiltrante resinoso contendo nanotubos de nitreto de boro (BNNTs). Infiltrantes contendo 90% de TEGDMA, 10% de Bis-GMA em massa e 1% CQ e EDAB em mol foram formulados. BNNTs foram adicionados aos infiltrantes nas concentrações de 0,1% e 0,2% em massa ( $I_{BNNT0,1\%}$  e  $I_{BNNT0,2\%}$ , respectivamente). Um grupo foi formulado sem a adição dos nanotubos ( $I_{CG}$ ). Os infiltrantes preparados foram avaliados quanto ao grau de conversão, citotoxicidade em relação a fibroblastos de polpa dentária e queratinócitos e deposição mineral imediata e após 7, 14 e 28 dias de imersão em solução de saliva artificial. Para verificação dos depósitos, foram realizadas análises de superfície em Microscópio Eletrônico de Varredura após 28 dias de imersão em saliva artificial. Num segundo momento, dentes bovinos foram desmineralizados e os infiltrantes foram aplicados em sua superfície para a avaliação dos ângulos de contato, energia livre de superfície, rugosidade superficial e colorimetria ( $\Delta E$ ). Os dados do grau de conversão, citotoxicidade, energia livre de superfície e rugosidade foram analisados estatisticamente por ANOVA de uma via e teste Tukey ( $p < 0,05$ ); os dados dos ângulos de contato e colorimetria foram avaliados estatisticamente por ANOVA de duas vias e teste Tukey ( $p < 0,05$ ). Análises descritivas foram realizadas para avaliação da deposição mineral e de imagens de microscopia eletrônica de varredura. Os valores de grau de conversão permaneceram entre 71,13% e 73,01% ( $I_{BNNT0,2\%}$  e  $I_{CG}$ , respectivamente). Todos os grupos apresentaram viabilidade celular acima de 70%. Houve deposição mineral com a adição de 0,1% e 0,2% BNNTs a partir de 7 dias de imersão em saliva artificial. Entre as diferentes concentrações de BNNTs, não houve diferença significativa do ângulo de contato, porém, a energia livre de superfície diminuiu de 60,84 mN/m ( $I_{CG}$ ) para 52,36 mN/M e 52,42 mN/m.

( $I_{BNNT0,1\%}$  e  $I_{BNNT0,1\%}$ , respectivamente). Houve diferença significativa para rugosidade superficial ( $p < 0,05$ ). Os resultados de  $\Delta E$  não apresentaram diferença estatística para o mesmo substrato. Conclui-se que a adição de BNNTs ao infiltrante resinoso induziu a deposição mineral sobre a superfície dos infiltrantes contendo BNNTs a partir de 7 dias de imersão em saliva artificial e diminuiu a energia livre de superfície sem alterar significativamente a cor do substrato.

## ABSTRACT

The aim of this study was to evaluate the properties of enamel resin infiltrants containing boron-nitride nanotubes (BNNTs). Resin infiltrants were compound by 90 wt.% TEGDMA, 10 wt.% Bis-GMA and 1 mol.% of each CQ and EDAB. BNNTs were added to the resin blend at 0.1 wt.% and 0.2 wt.% ( $I_{BNNT0.1\%}$  and  $I_{BNNT0.2\%}$ , respectively). Also, one group compound by the neat resin was evaluated ( $I_{CG}$ ). The degree of conversion, cytotoxicity to pulp fibroblasts and human keratinocytes and mineral deposition immediately and after 7, 14 and 28 days of immersion in artificial saliva was assessed. In order to evaluate the deposition features, images of the surface of the samples were taken with a scanning electron microscope after 28 days immersed in artificial saliva. Then, bovine incisors were extracted, demineralized and the resin infiltrants were applied to its surface in order to evaluate the contact angle, surface free energy, surface roughness and colour ( $\Delta E$ ). The degree of conversion, cytotoxicity, surface free energy and roughness were statistically assessed by one-way ANOVA and Tukey ( $p < 0.05$ ). The contact angles and surface colour were statistically assessed using two-way ANOVA and Tukey ( $p < 0.05$ ). Also, descriptive analysis was performed to the mineral deposition and scanning electron microscope images. The values of degree of conversion remained between 71.13% e 73.01% ( $I_{BNNT0.2\%}$  e  $I_{CG}$ , respectively). All groups showed cell viability over 70%. Mineral deposition occurred at the surface of samples containing 0.1 wt.% and 0.2 wt.% of BNNTs from 7 days of immersion. No statistical difference was observed for the contact angles, however, the surface free energy decreased from 60.84 mN/m ( $I_{CG}$ ) to 52.36 mN/M and 52.42 mN/m ( $I_{BNNT0.1\%}$  and  $I_{BNNT0.1\%}$ , respectively). Statistical difference was observed for the surface roughness between sound, demineralized and infiltrated enamel. The  $\Delta E$  showed no difference for

comparisons between the same baselines. As conclusions, the addition of BNNTs led to the mineral deposition over the samples from 7 days after immersion in artificial saliva and to a decrease of surface free energy without significant effect to the colour of the substrate.

## SUMÁRIO

<b>1 INTRODUÇÃO.....</b>	<b>13</b>
<b>2 OBJETIVO.....</b>	<b>21</b>
2.1 OBJETIVO GERAL.....	21
<b>3 ARTIGO.....</b>	<b>22</b>
3.1 ABSTRACT.....	24
3.2 INTRODUCTION.....	25
3.3 MATERIALS AND METHODS.....	26
3.4 RESULTS.....	30
3.5 DISCUSSION.....	31
3.6 CONCLUSION.....	35
3.7 REFERENCES.....	36
3.8 TABLES.....	41
3.9 IMAGES.....	42
<b>4 CONSIDERAÇÕES FINAIS.....</b>	<b>47</b>
<b>REFERÊNCIAS.....</b>	<b>52</b>

## **1 INTRODUÇÃO**

A cárie é a doença mais prevalente do mundo (Kassebaum *et al.*, 2015). A formação do biofilme é multifatorial e está associada ao metabolismo de carboidratos em ácidos orgânicos que dissolvem os minerais que compõem o esmalte e a dentina. Diferentemente da dentina, as lesões no esmalte dentário são caracterizadas pela existência de uma camada externa pseudo-intacta, enquanto a sua camada subsuperficial apresenta um perfil de maior porosidade (Paris *et al.*, 2013). Essa porosidade se configura como um caminho livre, pelo qual podem se difundir substâncias como ar e outros fluidos (Paris *et al.*, 2013). A partir do momento em que a região porosa se encontra preenchida por substâncias diferentes da apatita encontrada no esmalte, ocorre a difração heterogênea da luz visível, alterando o índice de refração (IR) do esmalte sadio ( $IR \approx 1,62$ ) (Paris *et al.*, 2013). Uma vez que a aparência do esmalte hígido é uma combinação de suas propriedades óticas, os diferentes IR da água e do ar (1,33 e 1,00, respectivamente) tem efeito sobre a translucência total da superfície, fazendo com que o substrato desmineralizado tenha uma aparência branca e opaca, se assemelhando a uma superfície dita como “*Chalky-like*” (Brodbelt *et al.*, 1981).

As lesões iniciais de cárie, comumente chamadas de lesões de mancha branca, podem ocorrer por diversos motivos, tais como o desenvolvimento de defeitos no esmalte ou pela utilização de aparelhos ortodônticos, que promovem, na superfície lisa do esmalte dentário, superfícies retentivas de placa bacteriana (Øgaard *et al.*, 1988). Atualmente, existem três diferentes tipos de tratamentos para lesões iniciais de cárie: não invasivos, microinvasivos e invasivos. Métodos invasivos, como a utilização de microabrasão combinado com ácido clorídrico para

remoção de áreas de pequena profundidade afetadas por cárie, ainda são utilizados e possuem eficácia já reportada (Waggoner *et al.*, 1989). Porém, em conjunto com a remoção do tecido lesionado, ocorre também a de parte do tecido saudável que poderia ser remineralizado (Waggoner *et al.*, 1989; Meireles *et al.*, 2009). O segundo tipo de tratamento (não invasivo) visa remineralizar a região desmineralizada por meio da utilização de agentes terapêuticos que contenham fosfato e cálcio biodisponível (CPP-ACP), ou por aplicação tópica de fluoreto (Cochrane *et al.*, 2010), sem que seja necessária a remoção de tecido. Apesar de as lesões de mancha branca apresentarem redução na sua fluorescência depois de terem sido tratadas com CPP-ACP, a redução não foi significativa quando comparada ao uso diário de dentífricos fluoretados durante 4 semanas (Bröchner *et al.*, 2011). Outra desvantagem desse tipo de tratamento é o impedimento da ação dos íons de flúor liberados pelo agente terapêutico, devido à camada pseudo-intacta da região mais externa da lesão, que bloqueia a passagem desses íons (Naumova *et al.*, 2012).

Como alternativa para os tratamentos invasivos e situações em que o tratamento não invasivo não é eficaz, os procedimentos microinvasivos são indicados. Esses procedimentos consistem no selamento mecânico das superfícies desmineralizadas (Schwendicke *et al.*, 2015) ou na infiltração do esmalte dentário por meio da aplicação de uma resina fotopolimerizável de baixa viscosidade (Paris e Meyer-Lueckel, 2010; Meyer-Lueckel *et al.*, 2012). Em 1975, os adesivos foram os primeiros materiais testados com o intuito de infiltrar e selar mecanicamente as lesões de mancha branca (Dayila *et al.*, 1975), porém, essas resinas não tem a capacidade de mimetizar a aparência natural do esmalte dentário (De Lacerda *et al.*,

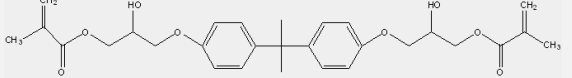
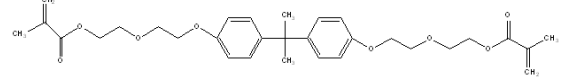
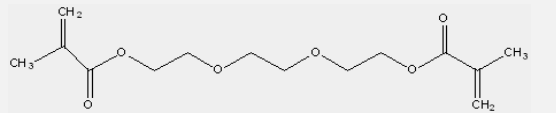
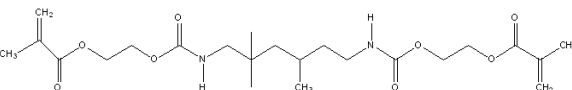
2016) e de penetrar suficientemente a região desmineralizada (Meyer-Lueckel *et al.*, 2006; Anauate-Netto *et al.*, 2017).

A aplicação dos infiltrantes de esmalte dentário não é realizada da mesma maneira que a de selantes ou adesivos. Os infiltrantes devem ser aplicados em duas etapas: 1) após o condicionamento ácido da superfície dentária, o infiltrante resinoso é aplicado, e seu excesso deve ser removido antes da primeira fotopolimerização; 2) após o preenchimento dos poros realizado durante a primeira etapa, o infiltrante deve ser reaplicado e novamente fotopolimerizado (Anauate-Netto *et al.*, 2017). A principal diferença entre os adesivos, selantes e infiltrantes está nas diferentes viscosidades dos monômeros que compõem a sua matriz polimérica, o que afeta diretamente na sua capacidade de penetrar (coeficiente de penetração) no substrato poroso originado pela desmineralização (Paris *et al.*, 2007a; Paschos, 2014).

O bis-fenol A-glicidil metacrilato (Bis-GMA) é um monômero bifuncional sintetizado pela primeira vez em 1965 por Rafael Bowen. No inicio, erroneamente se achava que esse componente poderia apresentar problemas à saúde devido ao seu precursor ser o bisfenol-A. Após verificada sua não toxicidade (Schmalz *et al.*, 1999), este tem sido amplamente utilizado em compósitos resinosos na Odontologia. O Bis-GMA possui alta massa molecular (MM) e viscosidade ( $\eta$ ) devido à existência de ligações aromáticas (anéis benzênicos) em sua estrutura e, por esse motivo, é comumente utilizado na presença de outro(s) monômero(s) menos viscoso(s) (Rueggeberg, 2002; Gonçalves *et al.*, 2009). Os comonômeros etoxilato bis-fenol A-glicol dimetacrilato (Bis-EMA), dimetacrilato de trietileno glicol (TEGDMA) e uretano dimetacrilato (UDMA) são opções que reduzem a viscosidade do Bis-GMA

e possibilitam também a adição de partículas de carga nas diferentes resinas compostas por ele (Gonçalves *et al.*, 2009). A tabela 1 mostra as características dos monômeros mencionados acima.

**Tabela 1:** Característica dos monômeros metacrilatos.

Monômero	MM (g·mol <sup>-1</sup> )	$\eta$ (Pa·s)	Estrutura Molecular
Bis-GMA	~512	~600~1000	
Bis-EMA	~540	~3	
TEGDMA	~286	~0,05	
UDMA	~470	~23	

Fonte: Elaborado pelo autor.

O coeficiente de penetração de um líquido é calculado pelo termo entre parênteses na equação de Washburn (**1**), que assume que uma superfície sólida e porosa (esmalte dentário desmineralizado) é um conjunto de capilaridades abertas, por onde um líquido (resina não fotopolimerizada) pode permear (Kirdponpattara *et al.*, 2013). Para a realização do cálculo do coeficiente de penetração, é necessário se conhecer a tensão de superfície entre o líquido e o ar ( $\gamma$ ), a viscosidade dinâmica da resina ( $\eta$ ) e o cosseno do ângulo de contato formado entre a superfície analisada e a resina infiltrada ( $\theta$ ).

$$d^2 = \left( \frac{\gamma \cos \theta}{2\eta} \right) rt \quad (1)$$

Quando os infiltrantes de esmalte dentário são aplicados sobre a lesão, a resina penetra o volume livre na região desmineralizada por forças capilares e oclui os poros, o que impede a progressão das lesões de estágio inicial (Paris *et al.*, 2007b; Gelani *et al.*, 2014). Apesar de o tratamento microinvasivo pela aplicação de infiltrantes resinosos ter sido desenvolvido para impedir o avanço de cárries iniciais, um outro efeito positivo do tratamento é o mascaramento da aparência opaca dessas lesões, melhorando a estética. Isso só é possível devido ao valor do IR da resina fotopolimerizável utilizada no tratamento de cárries incipientes apresentar valores muito próximos ( $IR \approx 1,51$ ) aos da hidroxiapatita ( $IR \approx 1,7$ ) (Borges *et al.*, 2013; Paris *et al.*, 2013).

Recentemente, estudos reportam a aplicação de infiltrantes resinosos para paralisação, ainda no estágio inicial, de lesões cariosas *in vitro* (Meyer-Lueckel *et al.*, 2016) e *in vivo* (Anauate-Netto *et al.*, 2017), havendo também trabalhos relacionados à capacidade dessas resinas de baixa viscosidade de camuflar a aparência não estética dessas lesões (Ceci *et al.*, 2017). Apesar desses infiltrantes apresentarem essas características, o material sozinho não possui nenhum efeito relacionado à remineralização do tecido adjacente, à proteção dessa região à posteriores desafios ácidos ou a mecanismos contra a adesão e crescimento de biofilme (Inagaki *et al.*, 2016a). Uma vez que tais mecanismos são interessantes para os infiltrantes de esmalte dentário, partículas de caráter antimicrobiano ou indutoras de deposição mineral vêm sendo adicionadas a essas resinas (Andrade Neto *et al.*, 2016; Inagaki *et al.*, 2016b; Sfalcin *et al.*, 2016).

Quanto a partículas com capacidade de induzir a deposição de mineral, um primeiro trabalho reportou a síntese, em laboratório, de nanobastões de

hidroxiapatita por método de coprecipitação hidrotérmica, com posterior adição à infiltrantes resinosos, tendo o objetivo de testar seu papel protetivo contra cárries recorrentes (Andrade Neto *et al.*, 2016). Uma quantidade de 10% em massa desses nanobastões resultou em um aumento da dureza Knoop quando comparado ao grupo controle, após a ciclagem de pH, mostrando um aumento da resistência do material a desafios ácidos que possam ocorrer depois da infiltração do esmalte dentário. Em outro estudo seguindo a mesma linha, partículas de β-fosfato tricálcio, fosfato amorfo, hidroxiapatita, biovidro 45S5 e biovidro dopado com zinco, foram adicionados a infiltrantes experimentais (Sfalcin *et al.*, 2016). Os materiais contendo partículas bioativas mostraram melhor desempenho em sorção, solubilidade e maiores valores de dureza, permitindo inferir a sua capacidade de remineralização. Em relação à adição de partículas com característica antimicrobiana, dois trabalhos foram publicados reportando a avaliação das propriedades biológicas, físicas e químicas de um infiltrante experimental contendo clorexidina em 0,1 e 0,2% em massa (Inagaki *et al.*, 2016a; Inagaki *et al.*, 2016b). Os grupos que continham o antimicrobiano apresentaram um halo de inibição significativamente maior contra *Streptococcus Mutans* do que os grupos que não continham o antimicrobiano. Além disso, as partículas adicionadas não tiveram relação com a alteração das propriedades físicas e químicas dos infiltrantes resinosos. Porém, a composição das blendas foi determinante para o efeito observado.

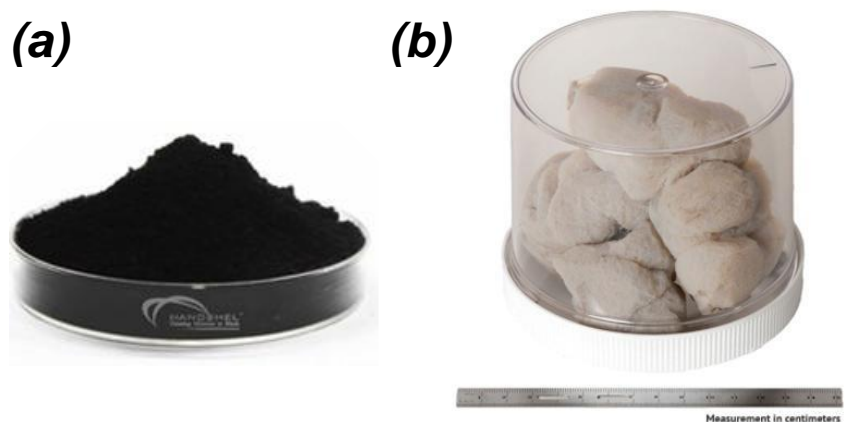
A adição de partículas objetivando a melhora das qualidades e das propriedades de biomateriais não é uma proposta nova (Bowen, 1963). Mas, na década de 90, com a descoberta dos nanotubos de carbono (CNTs) (Iijima, 1991), o campo de pesquisa acerca dos materiais de engenharia e biomateriais foi impulsionado. Os nanotubos são materiais de diâmetro nanométrico que se

assemelham a canudos, que possuem elevado volume interno e que podem ser funcionalizados por agentes químicos e/ou biomoléculas (Li *et al.*, 2013). Devido à versatilidade de rotas possíveis para sintetização (Rodriguez, 2011) e às excelentes propriedades dos CNTs, como alto módulo de elasticidade (Walters *et al.*, 1999), sua primeira aplicação na Odontologia se deu em resinas compostas (Zhang *et al.*, 2008). Porém, por apresentarem coloração cinza escura, a aparência do material restaurador foi considerada não estética, limitando a pesquisa desses nanotubos para utilização em materiais dentários. Anos depois, em 1995, foram sintetizados pela primeira vez os nanotubos de nitreto de boro (BNNTs) (Chopra *et al.*, 1995), de coloração branca-acinzentada, aumentando a possibilidade de aplicação dos nanotubo em Odontologia.

Os BNNTs são estruturas análogas dos CNTs, porém a sua cadeia molecular principal tem átomos de Boro (Br) e Nitrogênio (N) como substituintes da cadeia carbônica. Apesar das muitas similaridades, as propriedades físicas e químicas dos BNNTs diferem muito das dos CNTs. Apesar de apresentarem fundamentalmente ligações covalentes, devido à sua estrutura ser baseada em ligações com caráter levemente iônico entre os elementos B-N, os BNNTs são intrinsecamente piezoelétricos, o que não ocorre para o seu análogo (Yamakov *et al.*, 2017). Mecanicamente, as propriedades dos BNNTs são compatíveis às dos CNTs (Li *et al.*, 2017), além de possuírem maior inércia química (Yamakov *et al.*, 2017). Além dessas características, os BNNTs potencializam a hidrofobicidade das superfícies, têm biocompatibilidade com tecidos humanos, capacidade de funcionalização da sua superfície e também são suscetíveis à precipitação mineral quando expostos a soluções propícias (Gao e Xu, 2009). Todas essas características tornam os BNNTs muito atrativos no campo dos biomateriais, tendo sido sua primeira aplicação nessa

área como partícula de reforço em uma compósito à base da caprolactona (Lahiri et al., 2010). Recentemente, devido a sua aparência branco-acinzentada, os BNNTs foram testados como partículas biomiméticas em adesivos resinosos experimentais (Degrazia et al., 2017a; Degrazia et al., 2017b), sendo essa sua primeira aplicação em materiais dentários. A Figura 1 mostra as diferenças nas aparências entre os CNTs (a) e BNNTs (b).

**Figure 1:** Aspecto de CNTs (a) e BNNTs (b)



**Fonte:** [www.dir.indiamart.com](http://www.dir.indiamart.com) e [www.bnnt.org](http://www.bnnt.org)

Então, considerando as qualidades biomiméticas dos BNNTs, resta avaliar a possibilidade de sua utilização compondo, também, outros materiais de uso em Odontologia, como, por exemplo, os infiltrantes de esmalte dentário.

## **2 OBJETIVO**

### **2.1 OBJETIVO GERAL**

O objetivo do presente estudo foi formular um infiltrante experimental e avaliar a influência da adição de nanotubos de nitreto de boro nas suas propriedades.

### **3 ARTIGO**

Esta dissertação de mestrado se apresenta na forma de um manuscrito digitado nas normas do periódico *Dental Materials* para o qual foi submetido.

**Boron-nitride nanotubes as a novel filler to enamel infiltrants.**

Fabio Rocha Bohns

Universidade Federal do Rio Grande do Sul (UFRGS), Porto Alegre, Brazil.

Felipe Weidenbach Degrazia

Universidade Federal do Rio Grande do Sul (UFRGS), Porto Alegre, Brazil.

Vicente Castelo Branco Leitune

Universidade Federal do Rio Grande do Sul (UFRGS), Porto Alegre, Brazil.

Susana Maria Werner Samuel

Universidade Federal do Rio Grande do Sul (UFRGS), Porto Alegre, Brazil.

Fabrício Mezzomo Collares\*.

Universidade Federal do Rio Grande do Sul (UFRGS), Porto Alegre, Brazil.

\* Ramiro Barcelos, 2492 - LAMAD - Laboratório de Materiais Dentários. Bom Fim  
90035-003. Phone: +55 (51) 33085198 - Porto Alegre, RS – Brazil.

[fabricio.collares@ufrgs.br](mailto:fabricio.collares@ufrgs.br)

Acknowledgements:

The author would like to thanks CAPES – Brazil for the scholarship (F.R.B).

Conflict of Interest:

The authors deny any conflict of interest.

## ABSTRACT

Objectives: The aim of this study was to evaluate the properties of enamel resin infiltrants containing boron-nitride nanotubes (BNNTs). Methods: Resin infiltrants were compound by 90 wt.% TEGDMA, 10 wt.% Bis-GMA and 1 mol.% of each CQ and EDAB. BNNTs were added to the resin blend at 0.1 wt.% and 0.2 wt.% ( $I_{BNNT0.1\%}$  and  $I_{BNNT0.2\%}$ , respectively), remaining one groups with no addition of nanotubes ( $I_{CG}$ ). Resin discs were produced and the degree of conversion, cytotoxicity to fibroblasts and keratinocytes, the mineral deposition immediately and after 7, 14 and 28 days of immersion in artificial saliva were assessed. Scanning electron microscope images were taken from the samples after 28 days immersed in artificial saliva. Bovine incisors were extracted and immersed in demineralizing solution for 72 hours. Resin infiltrants were applied to their surface and the contact angle, surface free energy, surface roughness and colour were assessed. Results: The values of degree of conversion remained between 71.13% e 73.01% ( $I_{BNNT0.2\%}$  e  $I_{CG}$ , respectively). All groups showed cell viability over 70%. Mineral deposition occurred over samples containing 0.1 wt.% and 0.2 wt.% of BNNTs. No statistical difference was observed for the contact angles, however, the surface free energy decreased with the addition of BNNTs. The  $\Delta E$  showed no difference for comparisons between the same baselines. Statistical difference was observed for surface roughness. Significance: The addition of BNNTs to resin infiltrants showed mineral deposition and resulted in decreased surface free energy compared to the neat resin.

Keywords: Nanotubes; dental caries; dental enamel; hydrophobic and hydrophilic interactions; spectrum analysis, raman.

## **1. Introduction:**

White spot lesions (WSL) commonly occur due to bacterial activity, post-orthodontic decalcification of teeth, development of defect on enamel [1], or acidic food intake [2]. The lesions appear to be sound on the outer layer, followed by a more porous portion below [3]. Subsurface porosity act as a diffusion pathway to fluids and air [3], modifying the refractive index of sound enamel [4]. Non-invasive treatment of lesions by the application of bioavailable phosphate, calcium and fluoride ions has been proposed [5]. If the non-invasive treatment fails, the next step is based on a micro-invasive method of enamel infiltration with a low viscosity resin [6]. To date, the entombment and masking of initial caries lesions by capillary forces have been investigated [1, 3, 7-10]. Differently from pit and fissure sealants, enamel infiltration technique aims to penetrate the lesion body, creating a barrier to the progression of caries inside the enamel pores volume [7].

Enamel resin infiltrants (ERIs) are composed mainly by triethylene glycol dimethacrylate (TEGDMA), a monomer with low viscosity and related high penetration coefficient [2, 7, 10]. The infiltration of initial caries lesions with high TEGDMA content polymers have been shown to hamper the progression of non-cavitated lesions efficiently [11, 12]. Nevertheless, such infiltrants are unable to remineralize the adjacent restoration tissue and protect it from further acidic challenges [13]. Therefore, more than arrest, ERIs should induce marginal remineralization and reduce biofilm growth [14]. Hydroxyapatite nanorods, chlorexidine, amorphous calcium phosphates and bioglass have been added into ERIs in order to improve such properties [14-18]. To date, no study aimed to evaluate experimental infiltrants containing fillers that both promote biomimetic remineralization and reduce the surface wettability in order to decrease biofilm formation or retard microorganism colonization.

Boron-nitride nanotubes (BNNTs) are nanomaterials analogues to carbon nanotubes (CNTs), and were successfully synthesized by Chopra *et al.* in 1995 [19]. Due to its nanometric size, high surface/volume ratio, surface functionality, high elastic modulus, biocompatibility [20], hydrophobicity, chemical inertness and susceptibility to precipitation in aqueous media, BNNTs attracted attention as a filler to biomedical applications [21]. The apatite formation ability of BNNTs in physiological solution was showed [22], opening a broad gap of applications to the use of BNNTs in dentistry. Recently, BNNTs have been tested as biomimetic filler for resinous dental adhesive [23]. The objective of this study was to investigate the influence of the addition of BNNTs to the properties of a methacrylate-

based enamel infiltrants. The null hypothesis is that the incorporation of BNNTs to the resin matrix has no effect on its properties.

## 2. Materials and Methods:

### 2.1. Experimental infiltrants preparation:

Experimental infiltrants were prepared by mixing 90 wt.% of TEGDMA, 10 wt.% of bisphenol A-glycidyl methacrylate (Bis-GMA), 1 mol.% camphorquinone (CQ) and 1 mol.% of ethyl 4-dimethylaminebenzoate (EDAB), all obtained within Sigma Aldrich (Sigma Aldrich Co.; Jurubatuba, São Paulo, SP, Brazil). In order to formulate three experimental infiltrants, hexagonal boron-nitride nanotubes (BNNT; LLC, Newport News, VA, USA) with purity of ≈50%, average tube length of 200 µm, surface area of 212 m<sup>2</sup>/g and density of 0.5 g/L were added at two different concentrations of 0.1 wt.% or 0.2 wt.% ( $I_{BNNT0.1\%}$  and  $I_{BNNT0.2\%}$ , respectively), remaining one group with no addition of nanotubes ( $I_{CG}$ ). All materials were weighted with an analytical weighing-machine (AUW220D; Shimadzu, Kyoto, Japan). To allow complete homogeneity of the infiltrants, BNNTs were first ultrasonicated with Bis-GMA. Then, TEGDMA was added to the mixture, followed by CQ and EDAB with a final ultrassonication in darkness for 480 s.

### 2.2. Degree of conversion:

The degree of conversion (DC) of the infiltrants was evaluated in a Fourier-transform infrared spectrophotometer (FT-IR Vertex 70, Bruker Optics, Ettlingen, Germany) equipped with a attenuated total reflectance crystal (Platinum ATR-QL, Bruker Optics, Ettlingen, Germany). A small drop of the infiltrants was poured into a silicon mould measuring 10 mm in diameter and 2 mm thick ( $n = 3$ ) and spectra were assessed prior and after photo curing for 40 s with a 1200 mW/cm<sup>2</sup> (Radii Cal; SDI, Australia) 5 mm distant to the sample surface. DC was calculated using the intensities of aliphatic C=C peak at 1637 cm<sup>-1</sup> against an internal standard carbonyl group C=O peak at 1715 cm<sup>-1</sup> prior and after light-curing, following the formula:

$$DC(\%) = 100 \times \left( \frac{\text{peak height of cured aliphatic } C=C / \text{peak height of cured carbonyl } C=O}{\text{peak height of uncured aliphatic } C=C / \text{peak height of uncured carbonyl } C=O} \right)$$

### **2.3. Cytotoxicity sulforhodamine B (SRB) colorimetric assay:**

#### **Obtaining dental pulp fibroblasts**

Fibroblasts were obtained from an intact third molar with incomplete root formation of one patient without systematic health problems. The patient were asked to donate tooth for the study and, after the agreement, the Informed Consent (IC) was signed. Then, the tooth was immersed in 1 mL of Dulbecco's Modified Eagle Medium (DMEM), supplemented with Hepes, foetal bovine serum 10% (FBS) and 100 U/mL penicillin, 100 µg/mL streptomycin (Thermo Fischer Scientific, Waltham, Massachusetts, USA), at 37 °C and under 5% CO<sub>2</sub>/ 95% air atmosphere. After 24 h of pre-incubation period, the culture medium was changed every 2 days. Cell passages were performed after cells reached sufficient number.

#### **Obtaining human keratinocyte**

Immortalized human keratinocyte cell line HaCaT was obtained within Rio de Janeiro Cell Bank (BCRJ, Duque de Caxias, RJ, Brazil). Cells were immersed in DMEM complemented with 100 U/mL penicillin, 100 µg/mL streptomycin, 10% of FBS and 2 mM L-glutamine. Cells were cultured at 37 °C and under 5% CO<sub>2</sub>/ 95% air atmosphere. Every 3 days, cells received fresh medium and were sub cultured every 7 days.

#### **SRB cytotoxicity assay**

Fibroblasts obtained from human dental pulp and immortalized human keratinocyte were used for cytotoxicity analysis. Eluate were prepared by immersing infiltrant disks measuring 3 mm in diameter and 1 mm in height ( $n = 3$ ) into 1 mL of medium during 72 h. The cells were seeded in triplicate at a concentration of  $5 \times 10^3$  in 96 well plates and treated with 100 µL of eluate [24].

### **2.4. Mineral deposition:**

Mineral deposition was performed using micro-Raman spectroscopy (Senterra; Bruker Inc., Karlsruhe, Germany) equipped with a 100 mW diode laser. The system parameters were adjusted to 785 nm wavelength and spectral resolution of  $\approx 3.5 \text{ cm}^{-1}$  with 3 co-additions during 5 s. Resin discs measuring 4 mm in diameter and 2 mm in height of each infiltrants were used. Baseline measurements were taken from infiltrants discs. Then, one disc of each group was immersed in artificial saliva containing CaCl<sub>2</sub>·H<sub>2</sub>O, KH<sub>2</sub>PO<sub>4</sub>, KCl, and NaCl [25]. The reagents were dissolved in distilled water and buffered with tris-hydroxymethyl-aminomethane to a pH of approximately 9 and

then, the pH was adjusted to 7.05 using concentrated hydrochloric acid. After 7, 14 and 28 days of immersion, the phosphate peak of  $960\text{ cm}^{-1}$  were used to quantify the mineral deposition. A scanning electron microscope (JSM 6060, JEOL Ltd, Tokyo, Japan) set to a voltage of 3 kV, was used to evaluate the surface of samples after 28 days of immersion in artificial saliva.

## **2.5. Enamel slabs preparation:**

Specimens were prepared from extracted bovine permanent incisors, which were stored in distilled water for 7 days after extraction. The teeth were sectioned at the enamel-cementum junction using a water-cooled cutting wheel. The labial surface of the crowns were ground flat with silicon carbide sandpapers (600, 1200 and 2000 grit; Klingspor, Haiger, Germany), under water cooling until an area of at least 5 mm x 5 mm were produced. Then, the flat surfaces were polished (1- $\mu\text{m}$  alumina suspension; Fortel, São Paulo, SP, Brazil) in a polishing machine (Model 3v; Arotec, Cotia, SP, Brazil) under water cooling. Prior demineralization, each enamel surface was partially covered with acid-resistant nail varnish, leaving an open window measuring 5 mm x 5 mm. Initial caries lesion were created by subjecting the samples to a demineralizing solution as described previously by ten Cate and Duijsters [26], containing 2.2 mM  $\text{CaCl}_2$ , 2.2 mM  $\text{NaH}_2\text{PO}_4$ , 0.05 M acetic acid; the pH of the solution was adjusted with 1 M KOH to be 4.4. The solution was maintained at  $37^\circ\text{C}$  for 72 h and the pH was measured twice a day in a pHmeter (DM-22; Digimed, São Paulo, SP, Brazil) in order to secure that the pH continued constant. The samples were removed from the solution, cleaned with distilled water and dried with air jet. The teeth were then wear out to remove the nail varnish, remaining demineralized square-shaped blocks measuring 5 mm in length, 5 mm in width and 2 mm in height.

## **2.6. Enamel infiltration procedure:**

The enamel surfaces were etched with 37% phosphoric acid (Dentsply; Petrópolis, RJ, Brazil) for 30 s and rinsed with distilled water for 30 s. After air drying the demineralized enamel surface, the experimental infiltrants were gently applied with a microbrush (KG Sorensen; Cotia, SP, Brazil) for 30 s and then, thinned for  $\approx 2$  s with air jet with posterior light curing (Radii Cal; SDI, Australia) for 40 s. Three groups of test specimens were produced: infiltrated with resin with no addition of BNNTs ( $I_{CG}$ ), infiltrated with resin containing 0.1wt.% or 0.2 wt.% of BNNTs ( $I_{BNNT0.1\%}$  and  $I_{BNNT0.2\%}$ , respectively).

## **2.7. Contact angle and surface free energy:**

The contact angle (CA) was evaluated by sessile drop method using a camera based goniometer (Theta; Attension Biolin Scientific, Stockholm, Sweden). Approximately 1 $\mu$ L drop of each infiltrants was placed on sound and demineralized enamel blocks prepared as described previously (n = 5). After 10 s from the initial contact between the droplet and the sample ( $\theta$ ), an image was recorded and analysed with OneAttension software (Biolin Scientific, Stockholm, Sweden). Contact angles of each resin were calculated by the arithmetic mean between five measurements. Surface Free Energy (SFE) was analysed with OneAttension software (Biolin Scientific, Stockholm, Sweden) using images recorded after 10 s of contact, as described previously. Droplets of approximately 1 $\mu$ L of distilled water (polar liquid) and  $\alpha$ -bromonaphthalene ( $\alpha$ -Br) (dispersive liquid) were placed on the surface of infiltrated enamel blocks (n = 5). OWRK/Fowkes method [27, 28] (in mN/m) was used for SFE calculus purposes, following the formula:

$$\gamma_{ls} = \sigma_l + \sigma_s - 2 \left( \sqrt{\sigma_l^D \cdot \sigma_s^D} + \sqrt{\sigma_l^P \cdot \sigma_s^P} \right)$$

where  $\gamma_{ls}$  is the interfacial tension,  $\sigma_l$  is the liquid surface tension,  $\sigma_s$  is the solid surface tension,  $\sigma^D$  is the surface tension of the dispersive part and  $\sigma^P$  is the surface tension of the polar part. Different samples were used for each computed value in order to guarantee a surface free of contamination.

## **2.8. Surface roughness:**

Surface roughness test was carried out using a contact-type profilometer with a stylus (SJ-201; Mitutoyo, Santo Amaro, SP, Brazil). Sound, demineralized and infiltrated enamel blocks measuring 5 mm in length, 5 mm in width and 2 mm in height (n = 6) were used. Each specimen was put on a flat table and the profilometer needle was placed on the enamel block aligned to its surface. The values obtained were calculated by the arithmetic mean (Ra) of three analyses at different locations of each sample; 0.8 mm was used as cut-off length.

## **2.9. Colour assessment:**

Colour measurements were performed by a reflectance spectrophotometer (CARY 5000 UV-Vis-NIR; Agilent, Santa Clara, US) equipped with a DRA-1800 Integrating Sphere. The samples were positioned over a standard white background. A dark mask containing an opening measuring 4 mm in diameter was placed over the infiltrated surface to set the limits of analysis. The colour of each

sample was measured and quantified in terms of three coordinate values ( $L^*$ ,  $a^*$  and  $b^*$ ), as established by the Commission Internationale de l'Eclairage (CIE), which detects the colour of the sample in a three-dimensional space, regarding to its lightness, chroma and hue ( $n = 5$ ). The colour of the sound, demineralized and infiltrated enamel was assessed and recorded (M1, M2 and M3, respectively) under standardized conditions according to CIE  $L^*a^*b^*$  system. The differences on the parameters obtained ( $\Delta L^*$ ,  $\Delta a^*$  and  $\Delta b^*$ ) were calculated by M1, M2 and M3. Comparison between infiltrated enamel blocks colour and sound enamel (M1 x M3) and demineralized enamel (M2 x M3) were calculated. The overall changes in colour impression ( $\Delta E$ ) were calculated using the following formulas:

$$\Delta E1 = \sqrt{(LM3 - LM1)^2 + (aM3 - aM1)^2 + (bM3 - bM1)^2}$$

$$\Delta E2 = \sqrt{(LM3 - LM2)^2 + (aM3 - aM2)^2 + (bM3 - bM2)^2}$$

## **2.10. Statistical analysis:**

Statistical analysis was performed with SigmaPlot for Windows, version 12.0 (Systat Software, Inc. San Jose, CA, USA). The normality of data was evaluated using Shapiro-Wilk test ( $p \geq 0.05$ ). The degree of conversion, the cytotoxicity to human keratinocytes and dental pulp fibroblasts and the contact angles of water and  $\alpha$ -bromonaphthalene droplets over the specimens, the SFE and surface roughness data were analysed with one-way ANOVA and Tukey's test. The contact angles between resin infiltrants and enamel and colorimetry results were analysed using two-way ANOVA and Tukey's test. P values less than 5% were considered to be statistically significant. Also, descriptive analysis were performed on samples for micro-Raman and SEM images to evaluate the phosphate content after immersion of specimens in artificial saliva.

## **3. Results:**

The DC of experimental resin infiltrants are shown in Table 1. The  $I_{CG}$  reached a value of 73.01% of conversion, while the most concentrated group  $I_{0.2\%BNNT}$  reached 71.13%. The incorporation of BNNTs to the resin matrix induced no statistical difference to the results ( $p > 0.05$ ). Cytotoxic activities performed for both keratinocytes and dental pulp fibroblasts are shown in figure 1. The rate of survivability of all concentrations of BNNT for both lines of cells remained above 75%. No significant statistical difference was observed for pulp fibroblasts ( $p > 0.05$ ). Regarding keratinocytes, significant difference was observed in the group containing 0.2 wt.% of BNNTs ( $I_{0.2\%BNNT}$ ) in

comparison to less concentrated groups ( $p < 0.05$ ). Mineral deposition was found on specimens containing 0.1 wt.% and 0.2 wt.% of BNNTs after immersion in artificial saliva for 14 days and 7 days respectively.  $I_{0.2\%BNNT}$  showed the highest mineral content after 28 days of immersion (Fig. 2). Scanning electron microscopy images of the samples after 28 days in soaking media show mineral precipitation over BNNTs-containing groups (Fig. 3).

The contact angles of water and  $\alpha$ -bromonaphthalene droplets over infiltrated enamel blocks and the surface free energy results are represented in table 2. No statistical difference amongst groups was observed for both liquids ( $p > 0.05$ ). However, decrease on the surface free energy was found with the addition of 0.1 wt.% ( $52.36 \pm 3.48$ ) and 0.2 wt.% ( $52.42 \pm 1.61$ ) of BNNTs ( $p < 0.05$ ). The means and standard deviation values of experimental infiltrants droplets on sound and demineralized enamel surface are exhibited in figure 4. No significant difference was observed for droplets over the same surface ( $p > 0.05$ ). However, significant lower angles were acquired on demineralized surface ( $p < 0.05$ ). There was significant difference between the means of surface roughness ( $p < 0.05$ ) (table 1). Sound enamel showed the lowest surface roughness ( $0.86 \mu\text{m}$ ). Colorimetric results of infiltrated enamel calculated for both sound ( $\Delta E_1$ ) and demineralized ( $\Delta E_2$ ) baselines are represented in table 1. A small variation for both  $\Delta E_1$  and  $\Delta E_2$  was observed, with no difference intragroup. However, significant difference was found between sound and demineralized baselines for all groups ( $p < 0.05$ ).

#### 4. Discussion:

The addition of nanofillers has been related to induce several modifications to the properties of ERIs, such as DC [16] and bacterial penetration [29]. In this study, BNNTs were added into a resin blend containing TEGDMA and Bis-GMA. It is known that BNNTs' sidewalls displays affinity to chemical compounds containing aromatic groups due to  $\pi$ -stacking mechanism or hydrophobic interactions [30, 31]. The addition of BNNTs to the resin stimulated the mineral deposition after 7 days of immersion in artificial saliva and decrease in the SFE. Since the addition of the nanotubes had influenced the properties of ERIs, the null hypothesis must be rejected.

The percentage of consumption of double bonds during polymerization reaction is defined as the DC [32]. Since the addition of fillers may scatter and diffract light, the DC was evaluated [33]. The percentage of conversion of TEGDMA/Bis-GMA blends remained above 70% with the addition of BNNTs. Data found in literature regard the DC of rich TEGDMA (>80 wt.%) blends are discrepant.

Andrade Neto *et al.* [16] reported DC values of approximately 50% for neat infiltrants, while Araújo *et al.* [34] found DC over 60% and Inagaki *et al.* [14] reported values of DC around 60% for high TEGDMA-containing ERIs. Despite different composition of the resin blends, such results may be also due to the internal standard used to calculate the DC. As TEGDMA rich blends has monomers without aromatic carbon-carbon double bonds, the internal standard of  $1608\text{ cm}^{-1}$  have low intensity or is non-existent, being the carbonyl carbon-oxygen double bonds ( $1715\text{ cm}^{-1}$ ) a more reliable internal standard [35]. Moreover, the amount of remaining double bonds in the resin blends is also influenced by the filler size, geometry and type and to the nature of initiator system [36]. The photosensitizer system used in this research was CQ at 1 %.mol, which have been shown to be suitable for TEGDMA/Bis-GMA blends [35]. At the test conditions of this study, the addition of high surface area BNNTs did not influenced the DC of ERIs.

Despite the high DC, TEGDMA is related to be the major leachable in polymeric blends [37] showing lipophilic nature, which may easily pass through cellular membranes [38]. In addition, BNNTs present asbestos-like shape, which may suggest some degree of cytotoxicity to different cell lines depending on its concentration [39]. The cell viability of fibroblasts and keratinocytes to resin infiltrants were assessed.  $I_{BNNT0.2\%}$  showed the lowest cell viability when in contact to human keratinocytes; however, its cell viability is not on cytotoxic range [40]. This result suggests that the HaCaT cell line is more sensitive than fibroblasts to rich-TEGDMA polymeric blends containing BNNTs, since all concentrations reached levels of viability over 80%. Opposed to the findings of Horvath *et al.* [41], the asbestos-like shape of BNNTs at the concentrations used in this work, seems to presented no influence on the cytotoxicity of the resin blends against fibroblasts.

Enamel resin infiltration technique has been developed to close the gap between noninvasively and minimally invasive treatments on the early stages of dental caries [41]. It is well known [13] that the application of fluoride in combination with resin infiltrants is able to inhibit the progression of WSL and lessen the mineral loss of affected enamel. However, the application of fluoride requires a few recall of the patient to the dental office [16] and, in addition, the infiltrants alone is not able to prevent recurrent caries or to remineralize the adjacent tissue [13]. Thus, the addition of particles with biomimetic remineralization potential may be an appropriate method to improve the performance of infiltrants-enamel interface against the acidic challenge caused by oral bacteria. The apatite formation ability of BNNTs after 7, 14 and 28 days soaked in simulated body fluid was

reported [22]. Analogous to that, Degrazia *et al.* [23] showed the induction of mineral precipitation over the surface of adhesive samples containing BNNTs. In this study, increased intensity of Ca-P peaks ( $\approx 960 \text{ cm}^{-1}$ ) were observed over samples containing BNNTs from 7 to 28 days in artificial saliva. The potential of biomimetic materials saliva to nucleate Ca-P minerals when immersed in artificial is already known [25]. Since the deposition of amorphous apatite in simulated body fluid is due to the high ion concentration of the solution, we hypothesize that in artificial saliva it occurs likewise. At the first moment, the sample is covered with an amorphous apatite layer, which obstructs the direct contact of the apatite precipitates to the samples' surface. The second stage is the crystalline needles growth, which takes place as the ion concentration of the soaking media decreases [22]. This may explain the homogeneous deposition over the sample containing 0.2 wt.% BNNTs at 14 days in artificial saliva. No needle-like apatite structures were found over the samples by SEM. The growth of crystalline structures over BNNTs is reported for nanotubes soaked directly in contact to the media [22] or by controlling the grain size with application of spark plasma sintering [42]. However, the potential bottom-up biomimetic mineralization that occurred on the samples containing BNNTs could be a useful mechanism to remineralize the adjacent tissue, which may prolong the longevity of the resin and improve its performance against recurrent caries [16, 29, 43, 44].

The hydrophobicity is a remarkable and well documented property of BNNTs [21, 45-47]. In this study, BNNTs were added to ERIs and the contact angles and SFE were assessed. Both properties are key factors to the adhesion and penetration of the ERIs into enamel subporosities [7, 10, 17] and to the hydrolytic degradation of the polymer [48, 49]. Beyond that, the low surface energy of hydrophobic surfaces related reduced protein and bacterial attachment to substrates [50]. However, this relationship should be inferred carefully [51]. The addition of nanotubes seems to have no influence on the contact angles to both water and  $\alpha$ -bromonaphthalene. Infiltrants containing nanotubes showed small contact angles when dropped over demineralized enamel in comparison to sound surface. Also, its addition led to a decrease on the SFE. The wettability of rough surfaces was previously described by Wenzel [52]. These findings may suggest that the addition of BNNTs to ERIs do not affect its wetting capacity. Furthermore, the decrease on surface energy may enlighten a potential anti-adhesion property of the material [49]. However, further studies should be carried in

order to evaluate the biofilm formation over ERIs surface containing BNNTs to confirm this applicability.

More than just arrest the progression of initial caries lesions, the infiltration technique aim to mask the opaque colour of white spot lesions [1, 3, 8-10]. It is known that polymeric composites containing carbon nanotubes show to be grey-black coloured, which is not harmonious with natural teeth colour [53]. BNNTs are analogues to carbon nanotubes [19] but appear to be white-grey. Thus, the colour of infiltrated bovine enamel was evaluated and compared with sound ( $\Delta E1$ ) and demineralized ( $\Delta E2$ ) baselines. In relation to  $\Delta E$  means, the colour of infiltrated enamel remained unchanged, with or without nanotubes, to both substrates. However, low values of  $\Delta E1$  in comparison to  $\Delta E2$  were obtained. This result elucidates a small variation of colour between infiltrated and sound enamel than for infiltrated compared to demineralized enamel. The significant decreasing of  $L^*$  as well as increasing  $b^*$  values of resin infiltrants make the restoration to appear more like the sound enamel [3, 54]. It has been reported by Douglas *et al.* [55] that the greater the  $\Delta E$ , the high is the perceptibility and low the acceptability. The same work reports that the mean colour acceptability tolerance for 95% of observers was 4.0  $\Delta E$ . Taking this *in vivo* report into account, the results of  $\Delta E1$  obtained in this work are on the limits of tolerance. Thus, the white-grey colour of BNNTs seems to have no influence on the masking ability of resin infiltrants.

Great efforts have been made to improve the properties of dental polymers. Due to key properties such as susceptibility to precipitation in aqueous media and hydrophobicity, BNNTs attracted attention to its use in dentistry. As filler-free infiltrants do not stimulate the biomimetic remineralization of surrounding tissue, this work may shed a light onto enamel resin infiltrants with resistance to acidic challenges.

## **5. Conclusion:**

The addition of BNNTs at 0.1 wt.% and 0.2 wt.% to an experimental infiltrants, led to a mineral deposition over 28 days of immersion in artificial saliva and decrease in SFE. Also, its addition does not affect the DC or the masking potential of enamel resin infiltrants.

- [1] Kim S, Kim EY, Jeong TS, Kim JW. The evaluation of resin infiltration for masking labial enamel white spot lesions. *Int J Paediatr Dent*. 2011;21:241-8.
- [2] Gölz L, Simonis RA, Reichelt J, Stark H, Frentzen M, Allam J-P, et al. In vitro biocompatibility of ICON® and TEGDMA on human dental pulp stem cells. *Dent Mater*. 2016;32:1052-64.
- [3] Paris S, Schwendicke F, Keltsch J, Dorfer C, Meyer-Lueckel H. Masking of white spot lesions by resin infiltration in vitro. *J Dent*. 2013;41 Suppl 5:e28-34.
- [4] Brodbelt RH, O'Brien WJ, Fan PL, Frazer-Dib JG, Yu R. Translucency of human dental enamel. *J Dent Res*. 1981;60:1749-53.
- [5] Cochrane NJ, Cai F, Huq NL, Burrow MF, Reynolds EC. New approaches to enhanced remineralization of tooth enamel. *J Dent Res*. 2010;89:1187-97.
- [6] Aziznezhad M, Alaghemand H, Shahande Z, Pasdar N, Bijani A, Eslami A, et al. Comparison of the effect of resin infiltrant, fluoride varnish, and nano-hydroxyapatite paste on surface hardness and streptococcus mutans adhesion to artificial enamel lesions. *Electron Physician*. 2017;9:3934-42.
- [7] Paris S, Meyer-Lueckel H, Colfen H, Kielbassa AM. Penetration coefficients of commercially available and experimental composites intended to infiltrate enamel carious lesions. *Dent Mater*. 2007;23:742-8.
- [8] Bak S-Y, Kim Y-J, Hyun H-K. Color change of white spot lesions after resin infiltration. *Color Res Appl*. 2014;39:506-10.
- [9] Borges A, Caneppele T, Luz M, Pucci C, Torres C. Color Stability of Resin Used for Caries Infiltration After Exposure to Different Staining Solutions. *Oper Dent*. 2013.
- [10] Paris S, Meyer-Lueckel H, Ouml, Lfen H, Kielbassa AM. Resin Infiltration of Artificial Enamel Caries Lesions with Experimental Light Curing Resins. *Dent Mater J*. 2007;26:582-8.
- [11] Meyer-Lueckel H, Balbach A, Schikowsky C, Bitter K, Paris S. Pragmatic RCT on the Efficacy of Proximal Caries Infiltration. *J Dent Res*. 2016;95:531-6.
- [12] Meyer-Lueckel H, Bitter K, Paris S. Randomized controlled clinical trial on proximal caries infiltration: three-year follow-up. *Caries Res*. 2012;46:544-8.
- [13] Gelani R, Zandona AF, Lippert F, Kamocka MM, Eckert G. In vitro progression of artificial white spot lesions sealed with an infiltrant resin. *Oper Dent*. 2014;39:481-8.

- [14] Inagaki LT, Alonso RC, Araujo GA, de Souza-Junior EJ, Anibal PC, Hofling JF, et al. Effect of monomer blend and chlorhexidine-adding on physical, mechanical and biological properties of experimental infiltrants. *Dent Mater.* 2016;32:e307-e13.
- [15] Inagaki LT, Dainezi VB, Alonso RCB, Paula ABd, Garcia-Godoy F, Puppin-Rontani RM, et al. Evaluation of sorption/solubility, softening, flexural strength and elastic modulus of experimental resin blends with chlorhexidine. *J Dent.* 2016;49:40-5.
- [16] Andrade Neto DM, Carvalho EV, Rodrigues EA, Feitosa VP, Sauro S, Mele G, et al. Novel hydroxyapatite nanorods improve anti-caries efficacy of enamel infiltrants. *Dent Mater.* 2016;32:784-93.
- [17] Cibim DD IL, Dainezi VB, Pascon FM, Alonso RC, Kantoviz KR. Wettability Analysis of Experimental Resin-Infiltrants Containing Chlorhexidine. *Austin Dent Sci.* 2017;2.
- [18] Sfalcin RA, Correr AB, Morbidelli LR, Araújo TGF, Feitosa VP, Correr-Sobrinho L, et al. Influence of bioactive particles on the chemical-mechanical properties of experimental enamel resin infiltrants. *Clin Oral Invest.* 2016;1-9.
- [19] Chopra NG, Luyken RJ, Cherrey K, Crespi VH, Cohen ML, Louie SG, et al. Boron Nitride Nanotubes. *Science.* 1995;269:966-7.
- [20] Gao J, Xu B. Applications of nanomaterials inside cells. *Nano Today.* 2009;4:37-51.
- [21] Genchi GG, Ciofani G. Bioapplications of boron nitride nanotubes. *Nanomedicine.* 2015;10:3315-9.
- [22] Lahiri D, Singh V, Keshri AK, Seal S, Agarwal A. Apatite formability of boron nitride nanotubes. *Nanotechnology.* 2011;22:205601.
- [23] Degrazia FW, Leitune VCB, Samuel SMW, Collares FM. Boron nitride nanotubes as novel fillers for improving the properties of dental adhesives. *J Dent.* 2017;62:85-90.
- [24] Orellana EA, Kasinski AL. Sulforhodamine B (SRB) Assay in Cell Culture to Investigate Cell Proliferation. *Bio-protocol.* 2016;6.
- [25] Karlinsey RL, Hara AT, Yi K, Duhn CW. Bioactivity of novel self-assembled crystalline Nb<sub>2</sub>O<sub>5</sub> microstructures in simulated and human salivas. *Biomed Mater.* 2006;1:16-23.
- [26] ten Cate JM, Duijsters PP. Alternating demineralization and remineralization of artificial enamel lesions. *Caries Res.* 1982;16:201-10.
- [27] Fowkes FM. Attractive forces at interfaces. *Ind Eng Chem.* 1964;56:40-52.

- [28] Davis BW. Estimation of surface free energies of polymeric materials. *J Colloid Interface Sci.* 1977;59:420-8.
- [29] Khvostenko D, Hilton TJ, Ferracane JL, Mitchell JC, Kruzic JJ. Bioactive glass fillers reduce bacterial penetration into marginal gaps for composite restorations. *Dent Mater.* 2016;32:73-81.
- [30] Kim D, Sawada T, Zhi C, Bando Y, Golberg D, Serizawa T. Dispersion of boron nitride nanotubes in aqueous solution by simple aromatic molecules. *J Nanosci Nanotechnol.* 2014;14:3028-33.
- [31] Gao Z, Zhi C, Bando Y, Golberg D, Serizawa T. Noncovalent Functionalization of Disentangled Boron Nitride Nanotubes with Flavin Mononucleotides for Strong and Stable Visible-Light Emission in Aqueous Solution. *ACS Appl Mater Interfaces.* 2011;3:627-32.
- [32] Peutzfeldt A. Quantity of remaining double bonds of propanal-containing resins. *J Dent Res.* 1994;73:1657-62.
- [33] Leitune VCB, Collares FM, Trommer RM, Andrioli DG, Bergmann CP, Samuel SMW. The addition of nanostructured hydroxyapatite to an experimental adhesive resin. *J Dent.* 2013;41:321-7.
- [34] Araujo GS, Sfalcin RA, Araujo TG, Alonso RC, Puppin-Rontani RM. Evaluation of polymerization characteristics and penetration into enamel caries lesions of experimental infiltrants. *J Dent.* 2013;41:1014-9.
- [35] Collares FM, Portella FF, Leitune VCB, Samuel SMW. Discrepancies in degree of conversion measurements by FTIR. *Braz Oral Res.* 2014;28:9-15.
- [36] Ferracane JL, Greener EH. The effect of resin formulation on the degree of conversion and mechanical properties of dental restorative resins. *J Biomed Mat Res.* 1986;20:121-31.
- [37] Michelsen VB, Moe G, Strøm MB, Jensen E, Lygre H. Quantitative analysis of TEGDMA and HEMA eluted into saliva from two dental composites by use of GC/MS and tailor-made internal standards. *Dent Mater.* 2008;24:724-31.
- [38] Geurtsen W, Leyhausen G. Concise Review Biomaterials & Bioengineering: Chemical-Biological Interactions of the Resin Monomer Triethyleneglycol-dimethacrylate (TEGDMA). *J Dent Res.* 2001;80:2046-50.
- [39] Horvath L, Magrez A, Golberg D, Zhi C, Bando Y, Smajda R, et al. In vitro Investigation of the Cellular Toxicity of Boron Nitride Nanotubes. *ACS Nano.* 2011.
- [40] ISO 10993:5 Standard. Biological Evaluation of Medical Devices—Part 5: Tests for in vitro Cytotoxicity, 2009.

- [41] Paris S, Meyer-Lueckel H. Inhibition of caries progression by resin infiltration in situ. *Caries Res.* 2010;44:47-54.
- [42] Lahiri D, Singh V, Benaduce AP, Seal S, Kos L, Agarwal A. Boron nitride nanotube reinforced hydroxyapatite composite: Mechanical and tribological performance and in-vitro biocompatibility to osteoblasts. *J Mech Behav Biomed Mater.* 2011;4:44-56.
- [43] Kidd EAM, Beighton D. Prediction of Secondary Caries around Tooth-colored Restorations: A Clinical and Microbiological Study. *J Dent Res.* 1996;75:1942-6.
- [44] Altmann ASP, Collares FM, Balbinot GdS, Leitune VCB, Takimi AS, Samuel SMW. Niobium pentoxide phosphate invert glass as a mineralizing agent in an experimental orthodontic adhesive. *Angle Orthod.* 2017;87:759-65.
- [45] Kalay S, Yilmaz Z, Sen O, Emanet M, Kazanc E, Culha M. Synthesis of boron nitride nanotubes and their applications. *Beilstein J of Nanotechnol.* 2015;6:84-102.
- [46] Boinovich LB, Emelyanenko AM, Pashinin AS, Lee CH, Drelich J, Yap YK. Origins of thermodynamically stable superhydrophobicity of boron nitride nanotubes coatings. *Langmuir.* 2012;28:1206-16.
- [47] Li L, Li LH, Ramakrishnan S, Dai XJ, Nicholas K, Chen Y, et al. Controlling Wettability of Boron Nitride Nanotube Films and Improved Cell Proliferation. *J Phys Chem C.* 2012;116:18334-9.
- [48] Ito S, Hashimoto M, Wadgaonkar B, Svizer N, Carvalho RM, Yiu C, et al. Effects of resin hydrophilicity on water sorption and changes in modulus of elasticity. *Biomat.* 2005;26:6449-59.
- [49] Bourbia M, Ma D, Cvirkovitch DG, Santerre JP, Finer Y. Cariogenic bacteria degrade dental resin composites and adhesives. *J Dent Res.* 2013;92:989-94.
- [50] Chen M, Yu Q, Sun H. Novel Strategies for the Prevention and Treatment of Biofilm Related Infections. *Int J Mol Sci.* 2013;14:18488-501.
- [51] Liu Y, Zhao Q. Influence of surface energy of modified surfaces on bacterial adhesion. *Biophys Chem.* 2005;117:39-45.
- [52] Wenzel RN. Resistance of solid surfaces to wetting by water. *Ind Eng Chem.* 1936;28:988-94.
- [53] Zhang F, Xia Y, Xu L, Gu N. Surface modification and microstructure of single-walled carbon nanotubes for dental resin-based composites. *J Biomed Mat Res Appl Biomat.* 2008;86B:90-7.
- [54] Min JH, Inaba D, Kim BI. Evaluation of resin infiltration using quantitative light-induced fluorescence technology. *Photodiagnosis Photodyn Ther.* 2016;15:6-10.

[55] Douglas RD, Steinhauer TJ, Wee AG. Intraoral determination of the tolerance of dentists for perceptibility and acceptability of shade mismatch. *The Journal of Prosthetic Dentistry*. 2007;97:200-8.

Table 1: Results of the degree of conversion,  $\Delta E$  calculated using CIELab for sound ( $\Delta E1$ ) and demineralized ( $\Delta E2$ ) enamel and surface roughness with means and standard deviations of each group.

Groups	DC [%]	Sound ( $\Delta E1$ )	Demineralized	Surface
			( $\Delta E2$ )	Roughness ( $\mu m$ )
<b>Sound</b>	-	-	-	0.86 (0.28) <sup>A</sup>
<b>Demineralized</b>	-	-	-	3.06 (1.00) <sup>B</sup>
I <sub>CG</sub>	73.01 (5.57) <sup>A</sup>	4.04 ± 2.51 <sup>Aa</sup>	13.01 ± 4.09 <sup>Ab</sup>	2.36 (0.58) <sup>B</sup>
I <sub>0.1%BNNT</sub>	72.66 (2.25) <sup>A</sup>	4.34 ± 1.51 <sup>Aa</sup>	12.83 ± 2.17 <sup>Ab</sup>	2.42 (0.60) <sup>B</sup>
I <sub>0.2%BNNT</sub>	71.13 (2.95) <sup>A</sup>	4.09 ± 1.14 <sup>Aa</sup>	12.48 ± 4.17 <sup>Ab</sup>	2.44 (0.49) <sup>B</sup>

Different lowercase letter indicates statistical difference in the same row ( $p < 0.05$ ).

Different capital letter indicates statistical difference in the same column ( $p < 0.05$ ).

- Not evaluated.

Table 2: Values obtained for the contact angle of distilled water and  $\alpha$ -Br over specimens surface and SFE as means and standard deviation.

Groups	Contact Angle [ $\theta$ ]		SFE [mN/m]
	Water	$\alpha$ -Br	
I <sub>CG</sub>	45.67 (12.40) <sup>A</sup>	17.60 (5.51) <sup>A</sup>	60.84 (4.74) <sup>B</sup>
I <sub>0.1%BNNT</sub>	60.65 (11.57) <sup>A</sup>	13.67 (5.58) <sup>A</sup>	52.36 (3.48) <sup>A</sup>
I <sub>0.2%BNNT</sub>	55.59 (4.68) <sup>A</sup>	21.71 (5.03) <sup>A</sup>	52.42 (1.61) <sup>A</sup>

Different capital letter indicates statistical difference in the same column ( $p < 0.05$ ).

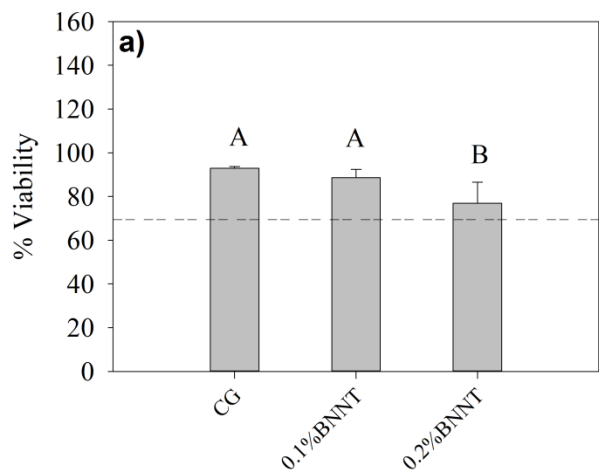
Figure 1: Cell viability (%) of experimental resin infiltrants against keratinocytes (a) and pulp fibroblasts (b) cell lines. The uppercase letters indicates significant statistical difference within each cell type.

Figure 2: Images obtained after the integration of the absorbance peak of  $\sim 960 \text{ cm}^{-1}$  on micro Raman spectrometer. Mineral deposits were found after 7 days of immersion in artificial saliva for the groups containing BNNTs. Increase of mineral deposition were found on the surface of experimental infiltrants containing higher amount of BNNTs concentration.

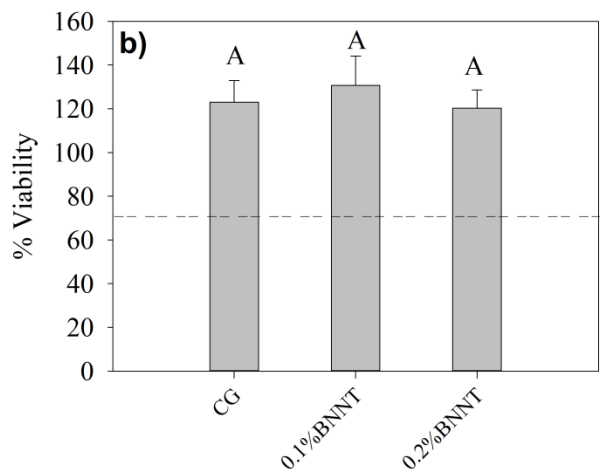
Figure 3: SEM images of the surface of samples after immersion in artificial saliva for 28 days. Mineral deposition was found over the surface of samples containing BNNTs.

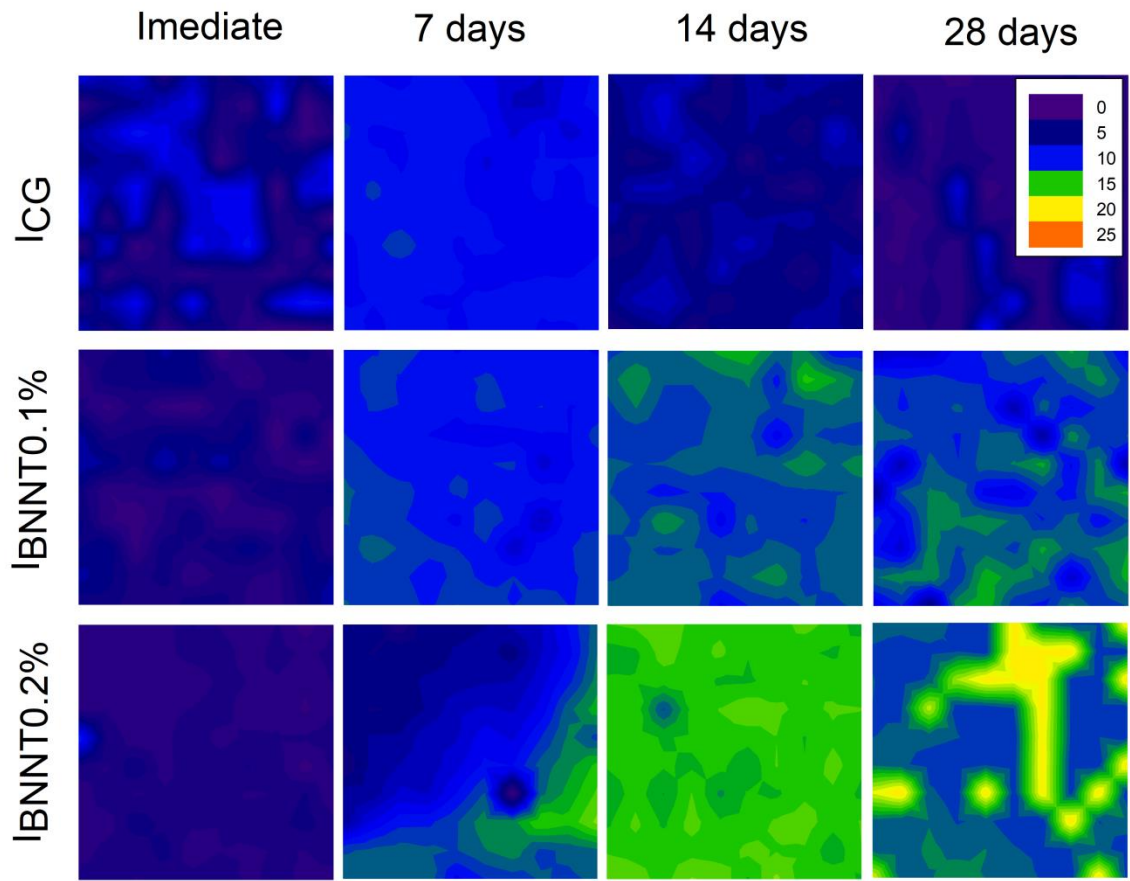
Figure 4: Contact angles ( $\theta$ ) of droplets of each experimental resin infiltrant over the surface of sound and demineralized enamel slabs. The uppercase letters indicates significant statistical difference within the same substrate. The small case letters indicates significant statistical difference between sound and demineralized surfaces.

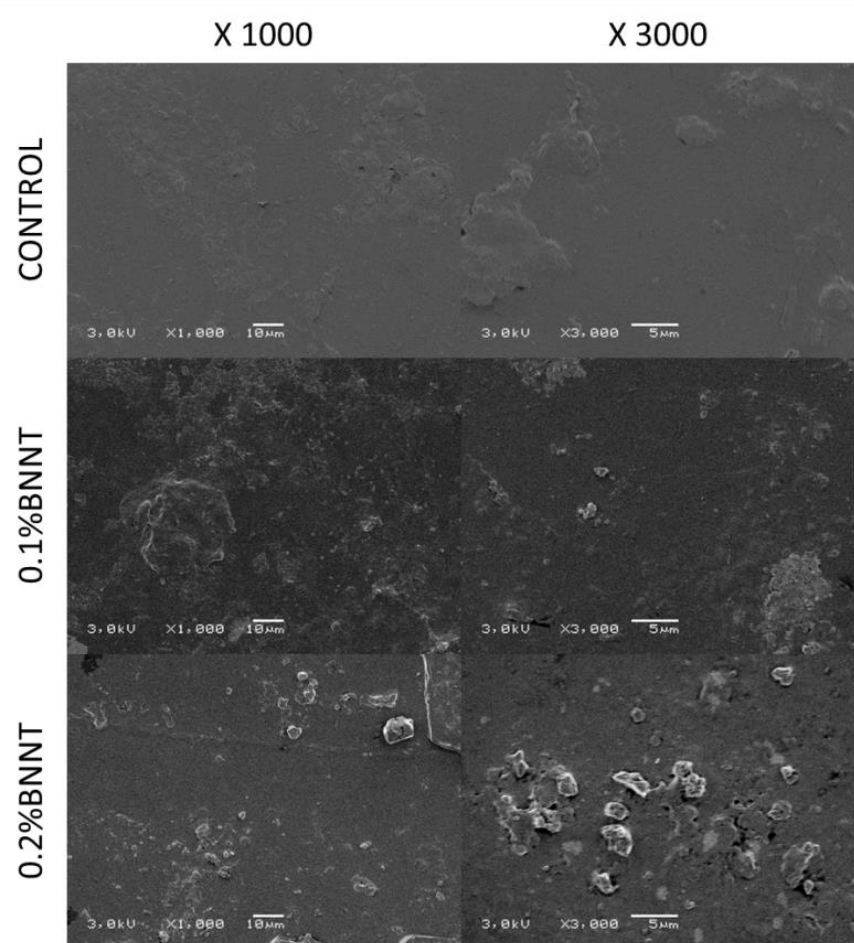
Keratinocytes

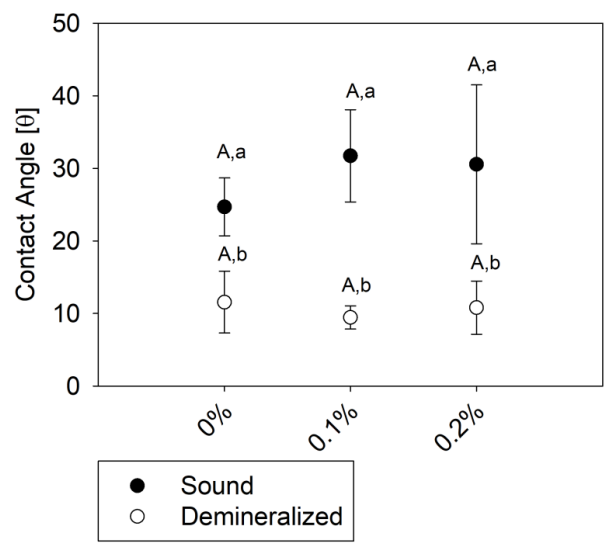


Pulp fibroblasts









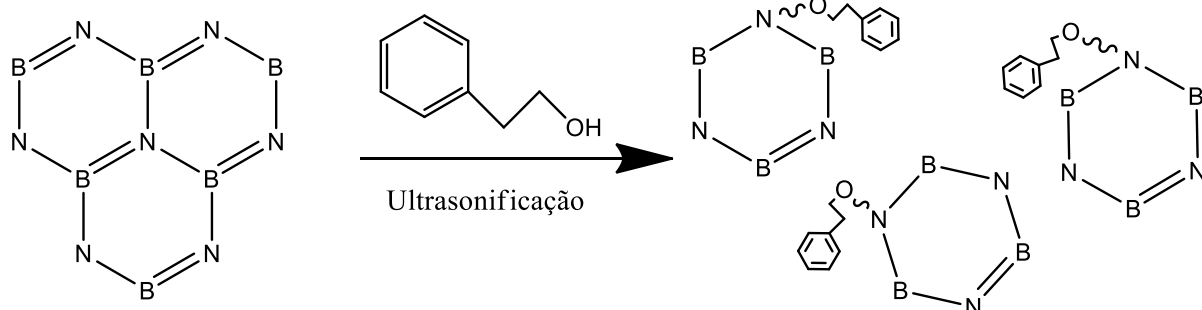
#### **4 CONSIDERAÇÕES FINAIS**

Com o surgimento de técnicas microinvasivas como alternativa para o tratamento de lesões de cárie iniciais, é possível a realização de um tratamento mais conservador, com menor remoção de tecido não afetado. Os infiltrantes de esmalte dentário são resinas fotopolimerizáveis de baixa viscosidade, que possuem a capacidade de penetrar os poros originados por um processo de desmineralização no substrato dentário (Paris *et al.*, 2007a; Paris *et al.*, 2007b). Quando a resina penetra esses poros por forças capilares e é fotopolimerizada, uma barreira contra possíveis desafios ácidos é estabelecida. Isso evita que as lesões iniciais (machas brancas) progridam para lesões cavitadas (Paris e Meyer-Lueckel, 2010). Acompanhamentos clínicos indicam a efetividade desses materiais em sustar a progressão das lesões (Anauate-Netto *et al.*, 2017). Porém, essas resinas se limitam a prevenir que as lesões avancem, não possuindo nenhum mecanismo que induza à remineralização marginal (Gelani *et al.*, 2014) ou que diminua a molhabilidade da superfície, para que a adesão e colonização de biofilme seja menor.

No presente estudo, nanotubos de nitreto de boro foram adicionados a uma resina contendo os monômeros TEGDMA e bis-GMA. Uma vez que os BNNTs possuem alta energia de superfície, após sua sintetização, encontram-se agregados e entrelaçados uns aos outros, como um novelo de lã (Kalay *et al.*, 2015). As paredes dos BNNTs são conhecidas por possuir afinidade química com compostos que contenham anéis benzênicos em sua estrutura, devido às interações do tipo π-π que ocorrem entre essas estruturas (Gao *et al.*, 2011; Kim *et al.*, 2014). A existência de anéis aromáticos na estrutura do Bis-GMA torna o monômero um excelente dispersante dos nanotubos, o que seria dificultado caso a composição do

infiltrante fosse somente pelo monômero TEGDMA. A Figura 2 mostra um esquema de como se dá o desentrelaçamento dos nanotubos quando adicionados a compostos que contenham anéis aromáticos em sua estrutura e uma energia externa é fornecida ao sistema.

**Figura 2 – Esquema representativo do desentrelaçamento dos BNNTs**



Fonte: Elaborado pelo autor.

Nas condições propostas neste trabalho, a adição de BNNTs ao infiltrante resinoso experimental não resultou em alteração do grau de conversão, da citotoxicidade em relação a fibroblastos, ângulo de contato, rugosidade superficial e coloração, induziu a deposição mineral e reduziu a energia livre de superfície, tendo os dois últimos ocorrido em ambas as concentrações.

O infiltrante resinoso experimental contendo 0,2% em massa de BNNTs apresentou viabilidade celular significativamente mais baixa do que a apresentada pelo grupo controle e pelo experimental contendo 0,1%. Apesar disso, esse valor não pode ser considerado citotóxico, pois permaneceu acima de 70% de viabilidade (ISO, 2009). Em relação às blendas poliméricas compostas majoritariamente por TEGDMA contendo BNNTs, os fibroblastos apresentaram maior resistência que os queratinócitos, uma vez que maiores valores de viabilidade foram encontrados para elas. A adição de BNNTs em biopolímeros foi reportada pela primeira vez por Lahiri e colaboradores, em 2011 (Lahiri *et al.*, 2011). Apesar de Lahiri ter avaliado a

capacidade dos nanotubos de induzir a precipitação mineral quando diretamente imersos em fluido corporal simulado (SBF), no presente trabalho os mecanismos de indução podem ser os mesmos: 1) ocorre a precipitação dos *flakes* de hidroxiapatita amorfna na extensão da superfície da amostra; 2) à medida que o tempo passa, ocorre a nucleação e o posterior crescimento de estruturas cristalinas *needle-like* de hidroxiapatita. Essas duas etapas poderiam explicar uma maior intensidade observada para o grupo mais concentrado (0,2% BNNT) em 28 dias de imersão em saliva artificial. Para verificação das estruturas, imagens das superfícies após 28 dias de imersão em saliva artificial foram capturadas com um microscópio eletrônico de varredura. Apesar de terem sido observadas estruturas de precipitados minerais, nenhuma estrutura do tipo *needle-like* foi observada. Contudo, a existência de precipitação mineral nos grupos contendo BNNTs em relação ao grupo controle no presente trabalho elucida o potencial biomimético desses compósitos.

Um infiltrante de esmalte dentário ideal, além de promover a remineralização do tecido adjacente, deve possuir um mecanismo que evite a adesão e colonização bacteriana à sua superfície, entretanto, sem prejudicar sua capacidade de penetração nos poros do esmalte desmineralizado. O ângulo de contato entre um líquido e uma superfície é uma das maneiras utilizadas para medir a capacidade de um infiltrante de molhar e penetrar nas porosidades do substrato desmineralizado (Paris *et al.*, 2007a; Cibim, 2017). Uma das propriedades mais marcantes dos BNNTs é a sua hidrofobicidade (Boinovich *et al.*, 2012). A natureza desse efeito hidrofóbico se dá basicamente por dois mecanismos: 1) a curvatura dos nanotubos e 2) sua alta energia de superfície. No primeiro mecanismo, quando aumentamos a curvatura de uma superfície, tornando-a convexa, aumentamos a área de ação da superfície, aumentando o ângulo de contato; já no segundo mecanismo, a alta

energia de superfície das ligações B-N faz com que uma maior quantidade de hidrocarbonetos seja adsorvida na superfície, aumentando, assim, o ângulo de contato. No presente estudo, não houve aumento significativo do ângulo de contato entre o infiltrante e o esmalte hígido ou desmineralizado, ou seja, a adição dos nanotubos parece não influenciar na molhabilidade do substrato. Por outro lado, houve alteração da energia livre de superfície das resinas contendo BNNTs. A relação entre a energia livre de superfície de um material e sua capacidade de ser colonizado por bactérias ainda não é bem estabelecida (Chen *et al.*, 2013), portanto, qualquer conclusão sobre o assunto deve ser feita com cautela (Bourbia *et al.*, 2013).

Além de impedir a progressão de lesões iniciais de cárie, os infiltrantes de esmalte dentário tem como função mascarar a aparência não estética dessas lesões (Paris *et al.*, 2013). Os BNNTs possuem aparência branco-acinzentada, tornando-os mais estéticos que os nanotubos de carbono. Essa melhor estética se demonstrou pela não alteração de coloração quando BNNTs foram adicionados à resina. Um material com  $\Delta E = 0$  não possui alteração de cor em relação ao seu comparativo e, consequentemente, quanto maior o  $\Delta E$ , maior a diferença entre os materiais (Douglas *et al.*, 2007). A literatura acerca do  $\Delta E$  de infiltrantes reporta valores bem variados, possivelmente pelos diferentes aparelhos e parâmetros utilizados (Borges *et al.*, 2013; Bak *et al.*, 2014). No presente estudo, a coloração das resinas com adição de nanotubos se manteve estável utilizando dentes bovinos hígidos como controle. E, em relação à utilização de superfícies desmineralizadas como comparação, os valores de  $\Delta E$  foram estatisticamente menores.

Sabendo das qualidades dos BNNTs e das diferentes propriedades que esses nanotubos podem oferecer aos materiais de uso odontológico, sua incorporação em infiltrantes de esmalte fornece funcionalidades que a resina pura não é capaz de fornecer, como indução de deposição mineral e menor energia livre de superfície. O campo de utilização dos BNNTs em Odontologia é atual e necessita de maior investigação. Quanto à sua relação com os infiltrantes resinosos, ainda são necessárias mais análises a respeito da capacidade de biofilmes aderirem e colonizarem sua superfície, assim como é necessária a mensuração dos fenômenos relacionados com a capacidade de penetrar o esmalte desmineralizado.

Com base nos resultados alcançados neste estudo e considerando as limitações do mesmo, os BNNTs apresentaram-se como promissores para serem utilizados como uma nova carga em infiltrantes resinosos de esmalte dentário.

## REFERÊNCIAS

ALTMANN, A. S. P. et al. Niobium pentoxide phosphate invert glass as a mineralizing agent in an experimental orthodontic adhesive. **Angle Orthod**, v. 87, n. 5, p. 759-765, 2017.

ANAUATE-NETTO, C. et al. Caries progression in non-cavitated fissures after infiltrant application: a 3-year follow-up of a randomized controlled clinical trial. **J Appl Oral Sci**, v. 25, n. 4, p. 442-454, Jul-Aug 2017.

ANDRADE NETO, D. M. et al. Novel hydroxyapatite nanorods improve anti-caries efficacy of enamel infiltrants. **Dent Mater**, v. 32, n. 6, p. 784-93, Jun 2016.

ARAUJO, G. S. et al. Evaluation of polymerization characteristics and penetration into enamel caries lesions of experimental infiltrants. **J Dent**, v. 41, n. 11, p. 1014-9, Nov 2013.

AZIZNEZHAD, M. et al. Comparison of the effect of resin infiltrant, fluoride varnish, and nano-hydroxy apatite paste on surface hardness and streptococcus mutans adhesion to artificial enamel lesions. **ElecPhys**, v. 9, n. 3, p. 3934-3942, Mar 2017.

BAK, S.-Y.; KIM, Y.-J.; HYUN, H.-K. Color change of white spot lesions after resin infiltration. **Color Res Appl**, v. 39, n. 5, p. 506-510, 2014.

BOINOVICH, L. B. et al. Origins of thermodynamically stable superhydrophobicity of boron nitride nanotubes coatings. **Langmuir**, v. 28, n. 2, p. 1206-16, Jan 17 2012.

BORGES, A. et al. Color Stability of Resin Used for Caries Infiltration After Exposure to Different Staining Solutions. **Oper Dent**, Dec 02 2013.

BOURBIA, M. et al. Cariogenic bacteria degrade dental resin composites and adhesives. **J Dent Res**, v. 92, n. 11, p. 989-94, Nov 2013.

BOWEN, R. L. Properties of a silica-reinforced polymer for dental restorations. **J Am Dent Assoc**, v. 66, p. 57-64, Jan 1963.

BRÖCHNER, A. et al. Treatment of post-orthodontic white spot lesions with casein phosphopeptide-stabilised amorphous calcium phosphate. **Clin Oral Invest**, v. 15, n. 3, p. 369-373, June 01 2011.

BRODBELT, R. H. et al. Translucency of human dental enamel. **J Dent Res**, v. 60, n. 10, p. 1749-53, Oct 1981.

0022-0345.

CECI, M. et al. Resin infiltrant for non-cavitated caries lesions: evaluation of color stability. **J Clin Exp Dent**, v. 9, n. 2, p. e231-e237, Feb 2017.

CHEN, M.; YU, Q.; SUN, H. Novel Strategies for the Prevention and Treatment of Biofilm Related Infections. **Int J Mol Sci**, v. 14, n. 9, p. 18488-18501, 2013.

CHOPRA, N. G. et al. Boron Nitride Nanotubes. **Science**, v. 269, n. 5226, p. 966-967, 1995.

CIBIM DD, I. L., DAINEZI VB, PASCON FM, ALONSO RC, KANTOVIZ KR. Wettability Analysis of Experimental Resin-Infiltrants Containing Chlorhexidine. **Austin Dent Sci.**, v. 2, n. (1), 2017.

COCHRANE, N. J. et al. New approaches to enhanced remineralization of tooth enamel. **J Dent Res**, v. 89, n. 11, p. 1187-97, Nov 2010.

COLLARES, F. M. et al. Discrepancies in degree of conversion measurements by FTIR. **Braz Oral Res**, v. 28, p. 9-15, 2014.

DAVIS, B. W. Estimation of surface free energies of polymeric materials. **J Colloid Interface Sci**, v. 59, n. 3, p. 420-428, 1977/05/01 1977.

DAYILA, J. M. et al. Adhesive Penetration in Human Artificial and Natural White Spots. **J Dent Res**, v. 54, n. 5, p. 999-1008, 1975.

DE LACERDA, A. J. et al. Adhesive Systems as an Alternative Material for Color Masking of White Spot Lesions: Do They Work? **J Adhes Dent**, v. 18, n. 1, p. 43-50, 2016.

DEGRAZIA, F. W. et al. Boron nitride nanotubes as novel fillers for improving the properties of dental adhesives. **J Dent**, v. 62, p. 85-90, 7// 2017a.

DEGRAZIA, F. W. et al. Long-term stability of dental adhesive incorporated by boron nitride nanotubes. **Dent Mater**, (article in press) 2017b.

DOUGLAS, R. D.; STEINHAUER, T. J.; WEE, A. G. Intraoral determination of the tolerance of dentists for perceptibility and acceptability of shade mismatch. **J Prosth Dent**, v. 97, n. 4, p. 200-208, 2007/04/01/ 2007.

FERRACANE, J. L.; GREENER, E. H. The effect of resin formulation on the degree of conversion and mechanical properties of dental restorative resins. **J Biomed Mater Res**, v. 20, n. 1, p. 121-31, Jan 1986.

FOWKES, F. M. ATTRACTIVE FORCES AT INTERFACES. **Ind Eng Chem**, v. 56, n. 12, p. 40-52, 1964/12/01 1964.

GAO, J.; XU, B. Applications of nanomaterials inside cells. **Nano Today**, v. 4, n. 1, p. 37-51, 2// 2009. ISSN 1748-0132.

GAO, Z. et al. Noncovalent Functionalization of Disentangled Boron Nitride Nanotubes with Flavin Mononucleotides for Strong and Stable Visible-Light Emission in Aqueous Solution. **ACS Appl Mat Interfaces**, v. 3, n. 3, p. 627-632, 2011/03/23 2011.

GELANI, R. et al. In vitro progression of artificial white spot lesions sealed with an infiltrant resin. **Oper Dent**, v. 39, n. 5, p. 481-8, Sep-Oct 2014.

GENCHI, G. G.; CIOFANI, G. Bioapplications of boron nitride nanotubes. **Nanomedicine**, v. 10, n. 22, p. 3315-9, Nov 2015.

GEURTSEN, W.; LEYHAUSEN, G. Concise Review Biomaterials & Bioengineering: Chemical-Biological Interactions of the Resin Monomer Triethyleneglycoldimethacrylate (TEGDMA). **J Dent Res**, v. 80, n. 12, p. 2046-2050, 2001.

GÖLZ, L. et al. In vitro biocompatibility of ICON® and TEGDMA on human dental pulp stem cells. **Dent Mater**, v. 32, n. 8, p. 1052-1064, 8// 2016.

GONCALVES, F. et al. Influence of BisGMA, TEGDMA, and BisEMA contents on viscosity, conversion, and flexural strength of experimental resins and composites. **Eur J Oral Sci**, v. 117, n. 4, p. 442-6, Aug 2009.

HORVATH, L. et al. In vitro Investigation of the Cellular Toxicity of Boron Nitride Nanotubes. **ACS Nano**, v. 5, n. 5, p. 3800-10, 2011.

IIJIMA, S. Helical microtubules of graphitic carbon. **Letters Nature**, v. 354, p. 56, 1991.

INAGAKI, L. T. et al. Effect of monomer blend and chlorhexidine-adding on physical, mechanical and biological properties of experimental infiltrants. **Dent Mater**, v. 32, n. 12, p. e307-e313, Dec 2016a.

INAGAKI, L. T. et al. Evaluation of sorption/solubility, softening, flexural strength and elastic modulus of experimental resin blends with chlorhexidine. **J Dent**, v. 49, p. 40-45, 6// 2016b.

**ISO 10993:5 Standard.** Biological Evaluation of Medical Devices—Part 5: Tests for in vitro Cytotoxicity, 2009.

ITO, S. et al. Effects of resin hydrophilicity on water sorption and changes in modulus of elasticity. **Biomaterials**, v. 26, n. 33, p. 6449-6459, 2005/11/01/ 2005.

KALAY, S. et al. Synthesis of boron nitride nanotubes and their applications. **Beilstein J Nanotechnol**, Trakehner Str. 7-9, 60487 Frankfurt am Main, Germany, v. 6, p. 84-102, 01/08, 2015.

KARLINSEY, R. L. et al. Bioactivity of novel self-assembled crystalline Nb<sub>2</sub>O<sub>5</sub> microstructures in simulated and human salivas. **Biomed Mater**, v. 1, n. 1, p. 16-23, Mar 2006.

KASSEBAUM, N. J. et al. Global burden of untreated caries: a systematic review and metaregression. **J Dent Res**, v. 94, n. 5, p. 650-8, May 2015.

KHVOSTENKO, D. et al. Bioactive glass fillers reduce bacterial penetration into marginal gaps for composite restorations. **Dent Mat**, v. 32, n. 1, p. 73-81, 1// 2016.

KIDD, E. A. M.; BEIGHTON, D. Prediction of Secondary Caries around Tooth-colored Restorations: A Clinical and Microbiological Study. **J Dent Res**, v. 75, n. 12, p. 1942-1946, 1996.

KIM, D. et al. Dispersion of boron nitride nanotubes in aqueous solution by simple aromatic molecules. **J Nanosci Nanotechnol**, v. 14, n. 4, p. 3028-33, Apr 2014.

KIM, S. et al. The evaluation of resin infiltration for masking labial enamel white spot lesions. **Int J Paediatr Dent**, v. 21, n. 4, p. 241-8, Jul 2011.

KIRDPONPATTARA, S.; PHISALAPHONG, M.; NEWBY, B.-M. Z. Applicability of Washburn capillary rise for determining contact angles of powders/porous materials. **J Colloid Interface Sci**, v. 397, n. Supplement C, p. 169-176, 2013.

LAHIRI, D. et al. Boron nitride nanotube reinforced polylactide-polycaprolactone copolymer composite: Mechanical properties and cytocompatibility with osteoblasts and macrophages in vitro. **Acta Biomat**, v. 6, n. 9, p. 3524-3533, 9// 2010.

LAHIRI, D. et al. Boron nitride nanotube reinforced hydroxyapatite composite: Mechanical and tribological performance and in-vitro biocompatibility to osteoblasts. **J Mech Behav Biomed Mat**, v. 4, n. 1, p. 44-56, 2011a.

LAHIRI, D. et al. Apatite formability of boron nitride nanotubes. **Nanotechnol**, v. 22, n. 20, p. 205601, May 2011b.

LEITUNE, V. C. B. et al. The addition of nanostructured hydroxyapatite to an experimental adhesive resin. **J Dent**, v. 41, n. 4, p. 321-327, 2013.

LI, L. et al. Controlling Wettability of Boron Nitride Nanotube Films and Improved Cell Proliferation. **J Phys Chem C**, v. 116, n. 34, p. 18334-18339, 2012.

LI, T. et al. A comparison between the mechanical and thermal properties of single-walled carbon nanotubes and boron nitride nanotubes. **Phys E Low-dim Syst Nanostruc**, v. 85, p. 137-142, 1// 2017.

LI, X. et al. The Use of Nanoscaled Fibers or Tubes to Improve Biocompatibility and Bioactivity of Biomedical Materials. **J Nanomat**, v. 2013, p. 16, 2013.

LIU, Y.; ZHAO, Q. Influence of surface energy of modified surfaces on bacterial adhesion. **Biophys Chem**, v. 117, n. 1, p. 39-45, Aug 2005.

MEIRELES, S. S. et al. Surface roughness and enamel loss with two microabrasion techniques. **J Contemp Dent Pract**, v. 10, n. 1, p. 58-65, Jan 2009.

MEYER-LUECKEL, H. et al. Pragmatic RCT on the Efficacy of Proximal Caries Infiltration. **J Dent Res**, v. 95, n. 5, p. 531-6, May 2016.

MEYER-LUECKEL, H.; BITTER, K.; PARIS, S. Randomized controlled clinical trial on proximal caries infiltration: three-year follow-up. **Caries Res**, v. 46, n. 6, p. 544-8, 2012.

MEYER-LUECKEL, H. et al. Influence of the application time on the penetration of different dental adhesives and a fissure sealant into artificial subsurface lesions in bovine enamel. **Dent Mat**, v. 22, n. 1, p. 22-28, 2006.

MICHELSEN, V. B. et al. Quantitative analysis of TEGDMA and HEMA eluted into saliva from two dental composites by use of GC/MS and tailor-made internal standards. **Dent Mat**, v. 24, n. 6, p. 724-731, 2008.

MIN, J. H.; INABA, D.; KIM, B. I. Evaluation of resin infiltration using quantitative light-induced fluorescence technology. **Photodiagnosis Photodyn Ther**, v. 15, p. 6-10, Sep 2016.

NAUMOVA, E. A. et al. Effects of different amine fluoride concentrations on enamel remineralization. **J Dent**, v. 40, n. 9, p. 750-755, 2012.

ØGAARD, B.; RØLLA, G.; ARENDS, J. Orthodontic appliances and enamel demineralization: Part 1. Lesion development. **Am J Orthod Dentofac Orthop**, v. 94, n. 1, p. 68-73, 1988.

ORELLANA, E. A.; KASINSKI, A. L. Sulforhodamine B (SRB) Assay in Cell Culture to Investigate Cell Proliferation. **Bio Protoc**, v. 6, n. 21, Nov 5 2016.

PARIS, S.; MEYER-LUECKEL, H. Inhibition of caries progression by resin infiltration in situ. **Caries Res**, v. 44, n. 1, p. 47-54, 2010.

PARIS, S. et al. Penetration coefficients of commercially available and experimental composites intended to infiltrate enamel carious lesions. **Dent Mater**, v. 23, n. 6, p. 742-8, Jun 2007a.

PARIS, S. et al. Resin Infiltration of Artificial Enamel Caries Lesions with Experimental Light Curing Resins. **Dent Mater J**, v. 26, n. 4, p. 582-588, 2007b.

PARIS, S. et al. Masking of white spot lesions by resin infiltration in vitro. **J Dent**, v. 41 Suppl 5, p. e28-34, Nov 2013. ISSN 0300-5712.

PASCHOS, E. Sealant and infiltrant penetration into pit and fissure caries lesions. **J Orof Ortho** v. 75, n. 5, p. 328-333, September 01 2014.

PEUTZFELDT, A. Quantity of remaining double bonds of propanal-containing resins. **J Dent Res**, v. 73, n. 10, p. 1657-62, Oct 1994.

RODRIGUEZ, N. M. A review of catalytically grown carbon nanofibers. **J Mat Res**, v. 8, n. 12, p. 3233-3250, 2011.

RUEGGEBERG, F. A. From vulcanite to vinyl, a history of resins in restorative dentistry. **J Prost Dent**, v. 87, n. 4, p. 364-379, 2002/04/01/ 2002.

CHMALZ, G.; PREISS, A.; ARENHOLT-BINDSLEV, D. Bisphenol-A content of resin monomers and related degradation products. **Clin Oral Investig**, v. 3, n. 3, p. 114-9, Sep 1999.

SCHWENDICKE, F. et al. Treating Pit-and-Fissure Caries:A Systematic Review and Network Meta-analysis. **J Dent Res**, v. 94, n. 4, p. 522-533, 2015.

SFALCIN, R. A. et al. Influence of bioactive particles on the chemical-mechanical properties of experimental enamel resin infiltrants. **Clin Oral Investig**, p. 1-9, 2016.

TEN CATE, J. M.; DUIJSTERS, P. P. Alternating demineralization and remineralization of artificial enamel lesions. **Caries Res**, v. 16, n. 3, p. 201-10, 1982.

WAGGONER, W. F. et al. Microabrasion of human enamel in vitro using hydrochloric acid and pumice. **Pediatr Dent**, v. 11, n. 4, p. 319-23, Dec 1989.

WALTERS, D. A. et al. Elastic strain of freely suspended single-wall carbon nanotube ropes. **Appl Phys Letters**, v. 74, n. 25, p. 3803-3805, 1999.

WENZEL, R. N. Resistance of solid surfaces to wetting by water. **Ind Eng Chem**, v. 28, n. 8, p. 988-994, 1936.

YAMAKOV, V. et al. Piezoelectric and elastic properties of multiwall boron-nitride nanotubes and their fibers: A molecular dynamics study. **Comput Mat Sci**, v. 135, n. Supplement C, p. 29-42, 2017.

ZHANG, F. et al. Surface modification and microstructure of single-walled carbon nanotubes for dental resin-based composites. **J Biomed Mater Res B Appl Biomater**, v. 86, n. 1, p. 90-7, Jul 2008.